

Original Article

Cite this article: Qi H, Chi Y, Sun L, Meng J, Wu P, Wei Z, Liu H, Wang Y, Liu R, and Xie Y. The effect of parent rocks on river sediment composition and implication for regional tectono-magmatic events: a case from two tributaries of the Songhua River, NE China. *Geological Magazine* 161(e24): 1–19. <https://doi.org/10.1017/S0016756824000517>

Received: 4 December 2023

Revised: 22 October 2024

Accepted: 12 November 2024

Keywords:

Lalin River; Jilin Songhua River; fluvial sediment; source control; source-sink process

Corresponding authors: Yunping Chi;




Email: 1982cyp@163.com,

Jie Meng; Email: mengjie26@126.com,

Yuanyun Xie; Email: xyy0451@163.com

*These authors contributed equally to this work.

The effect of parent rocks on river sediment composition and implication for regional tectono-magmatic events: a case from two tributaries of the Songhua River, NE China

Haodong Qi^{1,*}, Yunping Chi^{1,2} , Lei Sun^{1,2}, Jie Meng^{1,2} , Peng Wu³, Zhenyu Wei¹, Haijin Liu¹, Yehui Wang¹, Ruonan Liu¹ and Yuanyun Xie^{1,2,*} 

¹College of Geographic Science, Harbin Normal University, Harbin 150025, China; ²Heilongjiang Province Key Laboratory of Geographical Environment Monitoring and Spatial Information Service in Cold Regions, Harbin Normal University, Harbin 150025, China and ³School of Earth Sciences and Spatial Information Engineering, Hunan University of Science and Technology, Xiangtan, 411201, China

Abstract

Modern fluvial sediments provide important information about source-to-sink process and regional tectono-magmatic events in the source area, but many factors, e.g., chemical weathering, sedimentary cycles and source-rock types, can interfere with the establishment of the source-sink system. The Lalin River (LR) and the Jilin Songhua River (JSR) are two important tributaries of the Songhua River in the Songnen Plain in NE China. They have similar flow direction, topography and identical climate backgrounds, but have notably different parent-rock types in the headwater, which provides an opportunity to explore the influencing factors of river sediment composition. To this end, the point bar sediments in the two rivers were sampled for an analysis of geochemistry (including element and Sr-Nd isotopic ratios), heavy mineral and detrital zircon U-Pb dating. The results are indicative of the fact that the two rivers have the similar geochemical composition (e.g., elements and Sr isotopes) as well as chemical weathering (CIA = 51.41–57.60, CIW = 59.68–66.11, PIA = 51.95–60.23, WIP = 56.00–65.47, Rb/Sr = 0.38–0.42) and recycling (SiO₂/Al₂O₃ = 5.79 and 5.03, ICV = 1.0 and 1.2, CIA/WIP = 0.81–1.03) characteristics, showing a major control of climate on the low-level weathering and recycling of the river sediments. However, there are significant differences in the detrital zircon U-Pb age (a significant Mesozoic age peak for the LR but an additional Precambrian peak for the JSR), Nd isotope ratio (–6.2812–8.5830 and –8.1149–10.2411 for the LR and the JSR, respectively) and to a certain extent heavy mineral composition (e.g., for the < 63 μm fraction, a dominance of hornblende and magnetite in the LR, but haematite-limonite in the JSR) in the two river sediments, indicating that source rocks largely control the composition of the river sediments. Some of the major tectono-magmatic events (e.g., crustal growth and cratonisation of the North China Craton, closure of the Paleo-Asian Ocean, subduction and rollback of the Paleo-Pacific plate) occurring in the eastern Songnen Plain are well documented in the JSR sediments but not in the LR, the difference of which is largely regulated by the source rocks in the source area.

River is an important part of the surface morphology, and its sediments record rich information about the whole river basin (Kang et al., 2009; Yang et al., 2012; Zheng et al., 2013). The provenance tracing of river sediments is helpful to further understand the tectonic environment, paleoclimate, weathering process and drainage pattern during the sedimentary period, which is of great significance to the understanding of river source-sink system (Nesbitt and Young, 1982; Algeo and Maynard, 2004; Tribouillard et al., 2006; Hofer et al., 2013; Verma and Armstrong-Altrin, 2016; Zhang et al., 2019a, 2019b; Quek et al., 2021; Zhang et al., 2022a; Lin et al., 2022; Sun et al., 2022; Li et al., 2023a).

Provenance analysis, which allows for the diagnosis of the source areas of sediments and the establishment of relationships between source and sink areas through specific geological processes, has been widely used in many fields of the earth sciences (Weltje and Eynatten, 2004; Walsh et al., 2016; Sun et al., 2021; Wu et al., 2022). Because of their specific sources, the element geochemical characteristics of sediments can provide important information for deciphering their provenances, tectonic processes and environmental evolution (Yang et al., 2008; Singh, 2009; Clift et al., 2014); Sr-Nd isotopic composition, especially Nd isotope, is largely unaffected by geological processes and therefore has greater potential for determining sediment sources and transport patterns (Asahara et al., 2012; Lim et al., 2015; Carter et al., 2020); heavy minerals record in detail the characteristics of all geological events in the process of sediment transport from source to sink, and especially stable heavy minerals can be well preserved after physical and

© The Author(s), 2024. Published by Cambridge University Press. This is an Open Access article, distributed under the terms of the Creative Commons Attribution licence (<https://creativecommons.org/licenses/by/4.0/>), which permits unrestricted re-use, distribution and reproduction, provided the original article is properly cited.



chemical weathering, and thus can be used as one of the important indicators for provenance identification (Pettijohn et al., 1987; Mange and Wright, 2007; Yang et al., 2009); strong resistance to weathering and abrasion, as well as the ability to retain the characteristics of the source region, make the detrital zircon U-Pb dating widely used in sediment provenance tracing (Bao et al., 2013; Lin et al., 2020; Jones et al., 2022). However, it has been proved that a variety of factors, including chemical weathering, sedimentary cycle and source rock types, have a significant impact on the above indexes, which has caused great confusion and challenges for the establishment of large-scale drainage source-sink systems and provenance tracing study (Cao et al., 2019; Liyouck et al., 2023). In recent years, although the studies about the factors (chemical weathering, sedimentary recycling and source-area parent rock types) influencing composition of fluvial sediments have been performed in the process of the establishment of source-sink systems in many large drainage systems (Chi et al., 2021; Huyan and Yao, 2022; Huyan et al., 2023; Li et al., 2023a; Liyouck et al., 2023; Saha et al., 2023), but there is still a lack of relevant studies in Northeast China.

The Songhua River system is one of the most important rivers in Northeast China (Qiu et al., 2014; Wang et al., 2015a). As important tributaries of the Songhua River, the sediments of the Lalin River (LR) and the Jilin Songhua River (JSR) have a profound influence on the trunk Songhua River basin (Liu et al., 2013). The source tracing of river sediments is of unique value for the study and division of the basin-mountain coupling system (Matenco and Andriessen, 2013; Arató et al., 2021). The source areas of the two rivers are the Zhangguangcai Range and the Changbai Mountain, respectively, in which the strata of different ages and various types of parent rocks are interleaved. Accordingly, they are natural geological laboratory for studying the influence of various factors on the source-sink system during the process of sediment transport and deposition. Although the predecessors have studied the elements geochemistry of soil, surface water and groundwater as well as the control factors of the chemical weathering of the sediments in the LR and the JSR basins (Li, 2008; Liu et al., 2013; Wang et al., 2021), the various indicators have not yet been integrated to trace the source from the perspective of Quaternary geology. Instead, the limited studies focused on the discussion of soil, chemical weathering degree and element differentiation characteristics by element geochemical indexes (Li, 2008; Liu et al., 2013; Wang et al., 2021). Although Li (2010) employed detrital zircon U-Pb age and Hf isotope to study the sediment provenance of the JSR, only one index was selected, and the conclusion inevitably overlooked some information about the parent rock in the source area. At present, no conclusions have been drawn about the extent to which various factors influence the composition of the two river sediments in the process of transport and deposition.

To address the key scientific issues above, the river sediments of the LR and the JSR were selected for the analysis of element geochemistry (major, trace and rare earth elements), Sr-Nd isotopes, heavy minerals and zircon U-Pb dating data to compare the composition differences of the two river sediments with similar provenance areas but different parent-rock types. On this basis, the effects of chemical weathering, sedimentary cycle and parent rock composition on the river sediments are discussed. In addition, in order to reveal the tectono-magmatic events in the eastern Songnen Plain in geological past, we discuss the response of the detrital zircon U-Pb ages of the LR and the JSR sediments on crustal growth and cratonization of the North China Craton (NCC), the closure of the Paleo-Asian Ocean, subduction and

rollback of the Paleo-Pacific plate, respectively. This work is helpful to trace the provenance from source to sink in the basin-mountain coupled system and provides an important reference for the study of the Songhua River drainage evolution history.

1. Environmental setting

1. a. Physical geographical setting

The LR, a first-level tributary of the right bank of the trunk Songhua River (Gao et al., 1993), originates from the Shilazi Mountain at the west foot of the Beiyin Mountain in the Zhangguangcai Range, with a total length of 355 km and a drainage area of 2.18×10^4 km², runs from southeast to northwest and flows into the trunk Songhua River in Fuyu City (Fig. 1) (Wang et al., 2019).

The JSR originates from the Tianchi (41° 44' N, 124° 26' E), the main peak of the Changbai Mountain, with a total length of 958 km and a drainage area of 7.34×10^4 km², and flows into, from southeast to northwest, the trunk Songhua River in Songyuan city together with the Nenjiang River (Fig. 1) (Lv et al., 2017). The two rivers are located in the middle temperate zone and have a continental monsoon climate with an average annual temperature of 2.9–4.2°C and annual precipitation of 550–750 mm, mainly from June to September. In winter, the basin is under the control of the Siberian continental air mass, and the northwest monsoon prevails. In summer, it is affected by the southeast monsoon from the ocean often with heavy rain in that time (Zhou and Yu, 1984; Gao and Li, 2011).

1. b. Geological setting

Northeastern China (1,520,000 km²) is located in the eastern part of the Central Asian Orogenic Belt (CAOB) (Sengör et al., 1993; Wu et al., 1994; Jahn et al., 2000), at the junction of the NCC and the Siberian Craton (Fig. 2a) (Liu et al., 2021a; Liu et al., 2022), with widely exposed granite as its prominent feature (JBGMR, 1988; IMBGM, 1992; HBGMR, 1993). It is composed of several micro-continental blocks and suture zones between them (Fig. 2b, Wu et al., 2001; Li, 2010; Wang et al., 2022), and was significantly affected by the late Paleozoic closure of the Paleo-Asian Ocean and the Mesozoic Paleo-Pacific subduction and retreat (Wang and Mo, 1996; Wu et al., 2002; Wu et al., 2011; Liu et al., 2021a), as different from other regions in the CAOB.

The Songliao Basin was developed in the extensional tectonic environment, with a very high heat flow, and overlay the Songnen-Zhangguangcai Range Massif (SZRM) during Mesozoic (Ma 1987; Yang et al., 1997). Most of the basement of the Songliao Basin is composed of Paleozoic and Mesozoic substrata (Wu et al., 2001, 2002), and has the characteristics of thin crust (29–36 km thick) and thin lithosphere (60–80 km thick) (Ma 1987; Yang et al., 1996). The Changbai Mountain and Zhangguangcai Range are located on the eastern tectonic unit of the SZRM and span the Dunhua-Mishan, Solonker-Xar Moron-Changchun and Chifeng-Kaiyuan suture zones. The massive Triassic igneous rocks in the eastern SZRM and the western Jiamusi Massif were formed by bidirectional subduction of the Mudanjiang Ocean between the SZRM and Jiamusi Massif (Wang et al., 2012; Wei, 2012; Shao et al., 2013; Yang et al., 2014; Guo et al., 2015; Lv et al., 2015; Wang et al., 2015c; Yang et al., 2015; Zhao et al., 2018; Zhang et al., 2022b). The Zhangguangcai Range was formed by the subduction and subsequent overthrust of Silurian oceanic crust (Wang et al., 2012; Shao et al., 2013; Zhang et al., 2022b), and it has successively

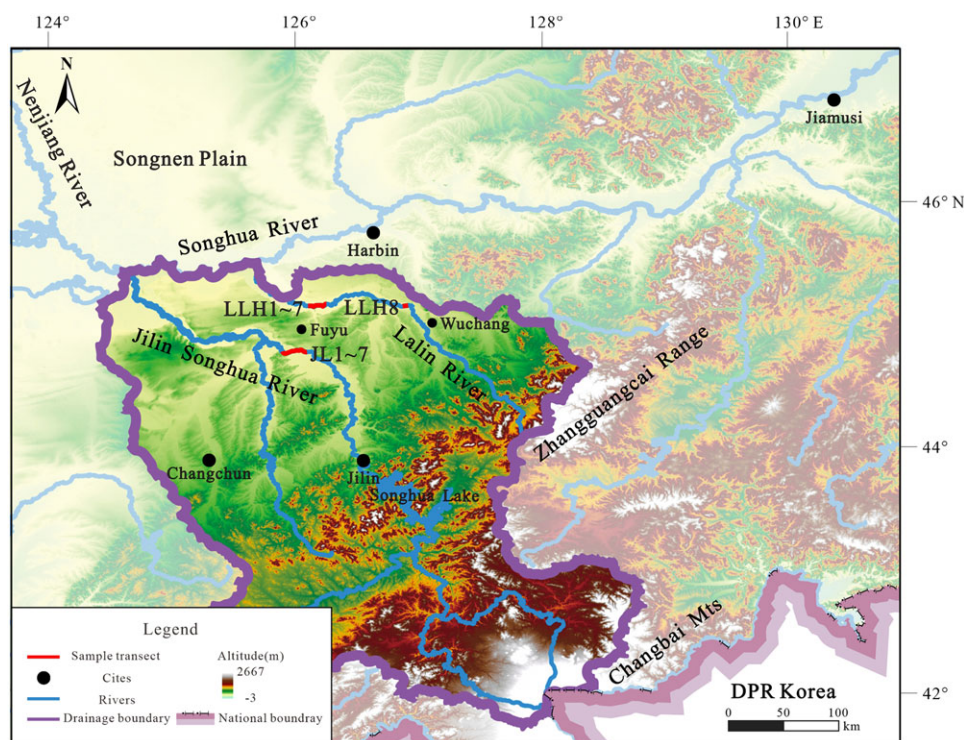


Figure 1. Digital elevation model map of the research area, showing the location of the sampling points and the basin range of the Lalin River and the Jilin Songhua River.

experienced an early arc magmatic stage (220–179 Ma) and a late metamorphic-deformation stage (193–165 Ma) (Shao et al., 2013). The formation of this orogenic belt marks the transition from the Mesozoic Paleo-Asiatic tectonic domain to the Pacific tectonic domain (Shao et al., 2013), and the existence of the granite in this area is also closely related to the collision event (Wu et al., 2011). The source rocks in the Zhangguangcai Range are mainly Triassic-Cretaceous intermediate-acid rocks (40.65%) and Devonian-Permian sandstone, conglomerate and granite (6.69%) (Fig. 2c and Table 1), with zircon U-Pb ages being in the range of Triassic (45.05%) and Jurassic (36.88%) period (Wu et al., 2011; Xu et al., 2013; Wang et al., 2015c).

The Changbai Mountain Range tectonically belongs to the terrigenous accretion belt on the northeast margin of the NCC (Qiao et al., 2016), and its source-rock types are mainly Triassic-Cretaceous intermediate-acid rocks (23.29%), Neoproterozoic granite-gneiss (8.50%), Cretaceous sand conglomerate, monzonite, conglomerate and volcanic rock (8.10%), Pleistocene basalt (7.74%) and Permian intermediate-felsic rocks and granite (6.46%) (Fig. 2c and Table 1). The zircons U-Pb ages of the Changbai Mountain Range are marked by a conspicuous Precambrian peak (about 51.40% of the total ages, especially 21.86% for 2.5 Ga), and meanwhile also show a considerable number of Paleozoic (29.77%) and Mesozoic (18.84%) ages (Wu et al., 2011; Wang et al., 2016b; Zhang et al., 2017). The Tianchi in the Changbai Mountain is a young bimodal volcano and is located in the uplifted area between the Songliao Basin and the Japan Sea back-arc basin (Liu et al., 2015), the uplift of which occurred during the middle-upper Pliocene to Pleistocene (Wang et al., 2003). It experienced three stages early shield formation (2–1 Ma), middle cone formation (1–0.02 Ma) and late eruption (Liu et al., 1998). A series of faulting and uplifting activities caused several eruptions of basaltic magma from the mantle magma chamber to the surface. After the volcanic eruption, a large area of basalt platform was formed around the Tianchi volcanic

cone (Horn and Schmincke, 2000; Wang et al., 2003; Siebert et al., 2010; Wei et al., 2013; Liu et al., 2015; Qiao et al., 2016).

2. Materials and methods

2. a. Sampling

The fine-grained components of river sand can represent the average composition in a large area after being strongly transported and mixed by wind and water power (Xie et al., 2019a, 2020). In order to constrain the sediment composition and provenance of the LR and the JSR, a total of 15 samples were obtained from the river point bars (Fig. 1), 7 from the JSR and the rest from the LR. All the samples obtained in this study are river sands near riverbed, lithologically different from the black soils through which the river flows, thus reflecting the composition of the source-area parent rocks. In addition, the samples are far away from urban population activity areas.

2. b. Analytical methods

In this paper, the obtained sediments were taken for elemental geochemistry, heavy mineral, Sr-Nd isotope and detrital zircon U-Pb dating analysis. After air-dried at room temperature, the bulk samples were dry-screened using standard sieve to obtain <63 μm fraction for element and Sr-Nd isotope analysis, <63 μm , 63–125 μm , 125–250 μm fractions for heavy mineral analysis and 63–250 μm fraction for U-Pb dating of detrital zircon.

2. b.1. Element geochemistry

Major elements were analyzed by a standard X-ray fluorescence spectrometer (AL104, PW2404) on fused glass beads. The detection limit is ~ 0.01 wt% and analytical precision (relative standard deviation) is <1%. Loss on ignition was obtained by weighing before and after 1 h of heating at 950 $^{\circ}\text{C}$. The tests for

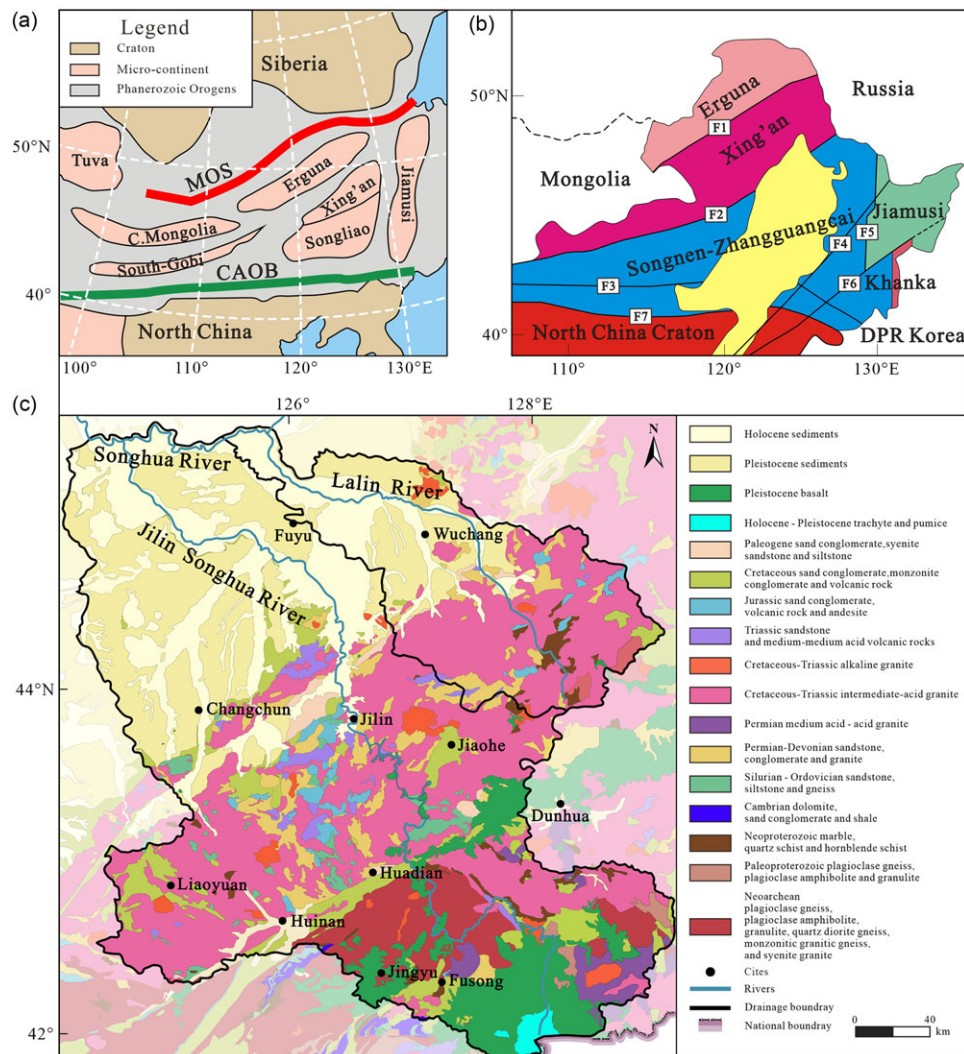


Figure 2. (a) Tectonic map of Northeast Asia (Wang et al., 2022). Abbreviations: CAOB = Central Asian Orogenic Belt; MOS = Mongol-Okhotsk Suture; C. = Central; (b) Tectonic division sketch map of NE China (Wu et al., 2011). F1 = Xinlin-Xiguitu Fault; F2 = Hegenshan-Heihe Fault; F3 = Solonker-Xar Moron-Changchun Fault; F4 = Yitong-Yilan Fault; F5 = Jiayin-Mudanjiang Fault; F6 = Dunhua-Mishan Fault; F7 = Chifeng-Kaiyuan Fault; (c) Geologic map of the source area of the Lalin River and the Jilin Songhua River, showing the basin range and the types of the source rocks.

trace and rare earth elements were performed by an inductively coupled plasma mass spectrometer (ICP-MS, Finnigan MAT ElementI) with relative standard deviations of less than $\pm 5\%$ and $\pm 1\%$, respectively. The external calibration was carried out by using Chinese National Standard soil reference samples (GSS-28). The sample pretreatment and testing of elemental geochemistry were carried out at the State Key Laboratory of Geological Processes and Mineral Resources, China University of Geosciences (Wuhan).

2. b.2. Heavy mineral analysis

Three grain-sized fractions ($<63 \mu\text{m}$, $63\text{--}125 \mu\text{m}$, $125\text{--}250 \mu\text{m}$) were used to characterize the heavy mineral composition of the LR and the JSR. The sub-samples were first weighed after drying in the oven of $<60^\circ\text{C}$, elutriated repeatedly with clear water in a washing pan for the removal of impurities and a dispersion of mineral grains and then separated with bromoform (density = 2.88) to collect heavy minerals. The collected heavy minerals were further separated, using magnetic and electromagnet methods, into diamagnetic, paramagnetic and ferrimagnetic groups, and then

weighed separately again. The identification for the heavy mineral groups was performed using stereomicroscopy and a polarized microscope, with identification numbers of each mineral species totalling up to 1000 grains. The weight percentage of heavy minerals was calculated. Details for heavy mineral analysis have been described by Xie et al. (2020). The pretreatment and heavy mineral analysis of the samples were carried out at Chengxin Geological Service Co., Ltd., Langfang City, Hebei Province, China.

2. b.3. Sr-Nd isotope

The sub-samples of $<63 \mu\text{m}$ fraction were soaked in 0.5 mol/L acetic acid solution at room temperature for 4h (Biscaye et al., 1997; Wang et al., 2007; Chen et al., 2007) in order to eliminate the influence of secondary carbonates on Sr isotope composition and ensure that only detrital minerals in sediments were analyzed (Wang et al., 2007; Újvári et al., 2012), and then dried and ground to 200 mesh. The Sr ($^{87}\text{Sr}/^{86}\text{Sr}$) and Nd ($^{143}\text{Nd}/^{144}\text{Nd}$) isotopic ratios were determined by thermal ionization mass spectrometry. The Sr and Nd isotopic ratios of the sub-samples were corrected for mass fractionation using $^{86}\text{Sr}/^{88}\text{Sr} = 0.1194$ and

Table 1. Areal percentages (%) of geological units in the Lalin River (LR) and Jilin Songhua River (JSR) catchments. The data here are calculated by ArcMap based on the digitized geological map of Northeast China and the digital elevation model.

Source rock types	LR	JSR
Holocene sediment	20.30%	14.70%
Pleistocene sediments	21.39%	15.03%
Pleistocene basalt	0.15%	7.74%
Holocene -Pleistocene trachyte and pumice	0.00%	0.60%
Paleogene sand conglomerate, syenite, sandstone and siltstone	2.29%	1.02%
Cretaceous sand conglomerate, monzonite, conglomerate and volcanic rock	1.42%	8.10%
Jurassic sand conglomerate, volcanic rock and andesite	1.55%	4.06%
Triassic sandstone and medium-medium acid volcanic rocks	0.37%	1.31%
Cretaceous-Triassic alkaline granite	1.22%	1.35%
Cretaceous-Triassic intermediate-acid granite	40.65%	23.29%
Permian medium acid - acid granite	0.00%	6.46%
Permian-Devonian sandstone, conglomerate and granite	6.69%	3.96%
Silurian - Ordovician sandstone, siltstone and gneiss	0.00%	1.25%
Cambrian dolomite, sand conglomerate and shale	0.00%	0.00%
Neoproterozoic marble, quartz schist and hornblende schist	2.40%	0.71%
Paleoproterozoic plagioclase gneiss, plagioclase amphibolite and granulite	0.00%	1.91%
Neoproterozoic plagioclase gneiss, plagioclase amphibolite, granulite, quartz diorite gneiss, monzonitic granitic gneiss and syenite granite	1.59%	8.50%

$^{146}\text{Nd}/^{144}\text{Nd} = 0.7219$, respectively. The accuracy of the instrument was tested with the international standard samples NBS987 and JMC, the measured values of which were $^{87}\text{Sr}/^{86}\text{Sr} = 0.710250 \pm 7$ (2σ) and $^{143}\text{Nd}/^{144}\text{Nd} = 0.512109 \pm 3$ (2σ), respectively. Chemical analysis blanks are <1 ng for Sr and <50 pg for Nd. The Nd isotopic composition is expressed by the $\epsilon_{\text{Nd}}(0)$ value, which is calculated as follows: $\epsilon_{\text{Nd}}(0) = \{[(^{143}\text{Nd}/^{144}\text{Nd})_{\text{sample}} / (^{143}\text{Nd}/^{144}\text{Nd})_{\text{CHUR}}] - 1\} \times 10000$.

Among them, $(^{143}\text{Nd}/^{144}\text{Nd})_{\text{CHUR}}$ uses the modern value of chondrite uniform reservoir (CHUR) values of $^{143}\text{Nd}/^{144}\text{Nd} = 0.512638$. The pretreatment and testing were carried out at the Key Laboratory of Mineral Resources in Western Gansu Province, Lanzhou University, China.

2. b.4. U-Pb dating of detrital zircon

Two 63–250 μm sub-samples were selected for zircon U-Pb dating. Zircon particles were extracted by conventional heavy liquid and magnetic separation methods, and then about 1000 grains were randomly selected by hand-picking under a binocular microscope. About 300 zircon particles were randomly selected to be fixed in epoxy discs and then polished to about half their thickness to expose its internal micro-structure. Transmitted electron, backscattered electron and cathode luminescence photographs were taken to observe their internal micro-textures. In the

process of selecting potential target spot sites for laser denudation, inclusions and fracture sites are avoided as much as possible. Due to the influence of crystallization temperature, magmatic zircons usually have oscillating rings, the different positions of which also affect the zircon ages (Hanchar and Miller, 1993; Corfu et al., 2003). Therefore, we try to avoid laser denudation points or ion beams passing through oscillating bands with different characteristics and choose bands with relatively uniform characteristics to avoid meaningless mixing ages (Wu and Zheng, 2004).

Zircon U-Pb dating was performed by laser denudation-inductively coupled plasma mass spectrometry (LA-ICP-MS) at the Key Laboratory of Mineral Resources in Western Gansu Province, Lanzhou University, China. The instrument was calibrated with the reference material NIST SRM 610 of synthetic silicate glass. The 91500 standard zircon and Plesovice (PLE) standard zircon were used as external and internal standards for age calibration monitoring (Wiedenbeck et al., 1995; Pearce et al., 1997; Sláma et al., 2008). The spot diameter is 30 μm , the denudation time is 40 s and the denudation depth is about 20 μm . The isotope ratio and element content data of the zircon grains were analyzed by Glitter 3.0 software, and the error of each age data was controlled within 1σ (Ludwig, 2003). The data of standard lead were calibrated by Andersen (Macro) (Andersen, 2002), and the Probability Density Plot and age histogram were drawn by Isoplot 3.0 programme (Ludwig, 2003). The $^{206}\text{Pb}/^{238}\text{U}$ and $^{207}\text{Pb}/^{235}\text{U}$ ages were used for ages younger and older than 1 Ga, respectively, and only ages with discordance within $\pm 10\%$ were accepted, resulting in a total of 257 zircons with concordant ages.

3. Results

3. a. Element geochemistry

3. a.1. Major elements

The major element distribution in the studied river sediments shows strong uniformity (Fig. 3a), but the contents of some major elements are slightly different. Specifically, the LR and JSR sediments contain similar contents of some major elements, such as SiO_2 (70.1–74.6% and 64.8–68.7%), Al_2O_3 (12.2–14.1% and 13.1–13.9%), Na_2O (3.0–3.7% and 2.5–3.1%), K_2O (2.8–3.0% and 2.9–3.1%), TiO_2 (0.6–0.8% and 0.7–1.0%), P_2O_5 (0.1–0.1% and 0.1–0.2%), FeO (0.8–1.4% and 0.7–1.5%). However, some major elements are different, such as Fe_2O_3 (2.2–3.2% and 4.1–5.2%), MgO (0.6–0.9% and 1.0–1.3%), CaO (1.5–1.9% and 1.7–3.5%), MnO (0.1–0.2% and 0.05–0.10%). Compared with Upper Continental Crust (UCC), SiO_2 contents in the sediments of the two rivers are similar, and TiO_2 and MnO are significantly enriched. Al_2O_3 , Na_2O and K_2O are slight losses, and MgO , CaO and P_2O_5 are significant losses. In the sediments of the two rivers, the depletion of Fe_2O_3 , MgO and CaO of the JSR sediments is smaller than that of the LR sediments, while the MnO content of the LR is significantly higher than that of the JSR. A detailed major element composition of the two river sediments is listed in Supplementary Table S1.

3. a.2. Trace elements

The characteristics of trace elements in the sediments of both the rivers show obvious similarities (Fig. 3b). Relative to UCC, the high field strength element Y (23.9–41.4 and 27.1–31.2 ppm for the LR and JSR, respectively, similarly hereinafter), Zr (273–1774 and 198–514 ppm), Th (7.5–19.7 and 10.8–18.2 ppm) are enriched in the LR and JSR sediments. Large ion lithophilic elements are

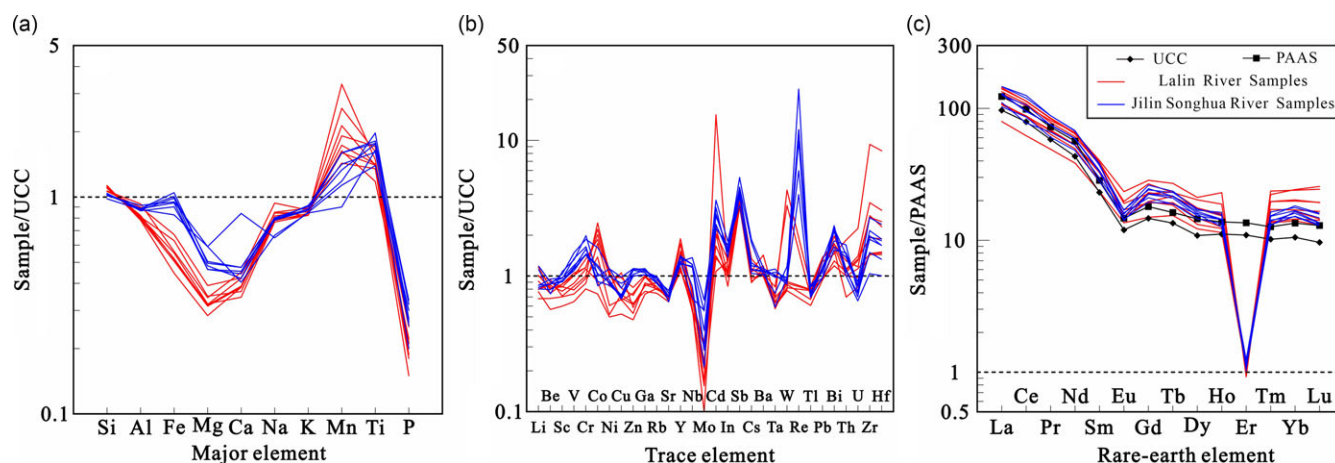


Figure 3. The normalized patterns for elements and chondrite-normalized rare earth element patterns for the Lalin River and Jilin Songhua River sediments. UCC and Post Archean Australian shale (PAAS) patterns are given as a reference. UCC, PAAS and chondrite values are after Taylor and McLennan (1985).

enriched in Cs (3.30–4.96 and 3.88–6.89 ppm), Ba (544–784 and 562–635 ppm) and Pb (18.7–27.4 and 19.3–25.8 ppm), and depleted in Rb (84–102 and 99–111 ppm) and Sr (226–253 and 226–274 ppm) in the sediments of the two rivers. Compared with UCC (1.50 ppm), the Mo (0.15–0.49 and 0.32–1.00 ppm) loss of both rivers is obvious. Compared with the JSR, the LR has significant loss of Nb (13.7–19.4 and 17.2–34.2 ppm), a slight loss of V (38.8–63.1 and 66.0–89.5 ppm) and Zn (33.8–58.5 and 71.3–80.8 ppm) and an enrichment of U (2.32–6.28 and 1.84–2.54 ppm). A detailed trace element composition of the river sediments is listed in Supplementary Table S1.

3. a.3. Rare earth elements (REE)

The contents of total rare earth elements (Σ REE) in the sediments are 125–223 ppm for the LR and 163–227 ppm for the JSR, higher than those in UCC (146 ppm) and PAAS (Post Archean Australian shale, 185 ppm). The patterns of rare earth elements in the two rivers are similar to those in UCC and PAAS, and show a right-leaning pattern (that is, 'the left side is steep and the right side is slow' trend, with $(\text{La}/\text{Yb})_N$ values of 5.5–7.7 for the LR and 6.2–9.2 for the JSR), showing enrichment of light rare earth elements (110–195 ppm for the LR and 143–206 ppm for the JSR), depletion of heavy rare earth elements (16–28 ppm for the LR and 19–22 ppm for the JSR) and significant negative Eu anomaly (0.50–0.71 for the LR and 0.50–0.64 for the JSR), as indicated in the chondrite-normalized REE patterns (Fig. 3c). The Ce anomalies are not clear with the values of 0.97–1.0 for the LR and 0.88–1.1 for the JSR. A detailed rare earth element composition of the two rivers is listed in Supplementary Table S1.

3. b. Heavy mineral

In total, 15 types of heavy minerals were detected in the two river sediments, including zircon, apatite, rutile, anatase, leucosene, titanite, hornblende, tourmaline, garnet, epidote, pyroxene, ilmenite and ferromagnetic minerals (haematite-limonite, magnetite, magnetic haematite), etc. A detailed heavy mineral composition of the <63 μm , 63–125 μm and 125–250 μm is listed in Supplementary Table S2. The heavy mineral composition is very different in the two rivers and in different grain-sized fractions (Fig. 4). In the <63 μm fraction, the LR consists mainly of hornblende (44.02%) and epidote (13.50%), followed by zircon (11.01%) and magnetite (8.03%), and other minerals account for

23.44%; the JSR is dominant in haematite-limonite (29.19%), magnetic haematite (18.44%), epidote (16.87%) and hornblende (13.12%). In the 63–125 μm fraction, hornblende in the LR increases significantly up to 65.42%, while the JSR is dominated by hornblende (37.63%) and epidote (25.87%). In the 125–250 μm fraction, hornblende occupies an absolute dominance (73.95%) in the LR, and the JSR has a higher content of hornblende (52.67%) and epidote (28.23%).

3. c. Sr-Nd isotopic composition

The $^{87}\text{Sr}/^{86}\text{Sr}$ ratios in the LR and JSR sediments are similar, with a value of 0.7099–0.7106 and 0.7105–0.7112, respectively. The ϵ_{Nd} (0) values can distinguish well among the two river sediments, -6.2812 – -8.5831 for the LR and -8.1149 to -10.2411 for the JSR (Fig. 5). A detailed Sr-Nd isotopic composition of two rivers is listed in Supplementary Table S1.

3. d. U-Pb dating of detrital zircon

Th/U ratios of most of the zircons are >0.1 (Fig. 6), indicating their magmatic origin, and a total of 257 zircon grains with Concordia ages were produced (Fig. 7). The zircon age patterns of the two rivers are clearly different (Fig. 8a–d). Specifically, the zircon ages of the LR sediments are mainly Mesozoic and Paleozoic (66–252 Ma, 252–541 Ma), whereas, in addition to the Mesozoic and Paleozoic zircons, a considerable number (36.92%) of Paleoproterozoic and Neoproterozoic (1.6–2.5 Ga, 2.5–2.8 Ga) zircons occur in the JSR sediments, suggesting their notably different age of the parent rocks in the sediment source areas. A detailed U-Pb dating of detrital zircon of the river sediments is listed in Supplementary Tables S3 and S4, respectively.

4. Discussion

4. a. Effects of chemical weathering on the river sediments

The element geochemical composition of sediments has been widely used in exploring the parent-rock types and provenance tracing of source areas (Cox et al., 1995; Jahn et al., 2001; Ding et al., 2001), but the composition can be affected by chemical weathering and even suffers alteration (Shao et al., 2012; Clift et al., 2014; Li et al., 2019). Therefore, it is necessary to evaluate the effects of chemical weathering on the geochemical indices of sediments

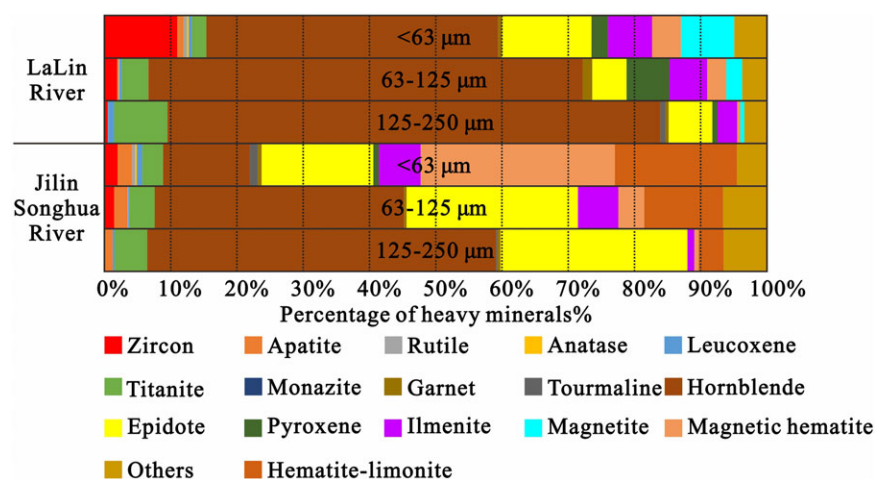


Figure 4. Heavy mineral abundances of the Lalin River and Jilin Songhua River sediments at <63 μm , 63–125 μm and 125–250 μm fractions, expressed as relative weight percentage (wt%).

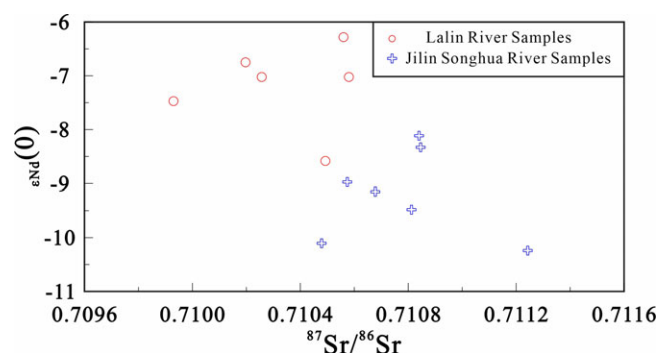


Figure 5. Sr-Nd isotopic composition in the Lalin River and Jilin Songhua River sediments.

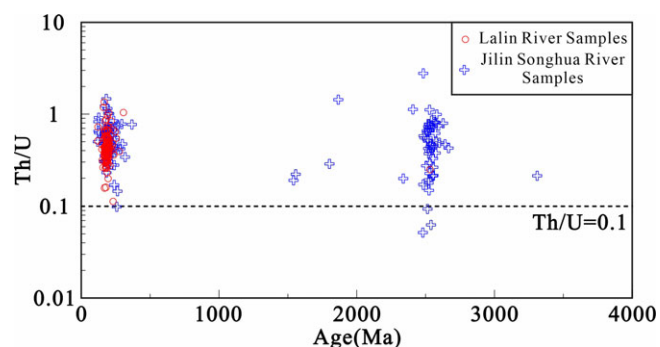


Figure 6. Diagram of zircon ages vs. Th/U ratios from the Lalin River and the Jilin Songhua River. The high Th/U ratios (>0.1) of most of the analyzed zircons suggest a magmatic source, while the low Th/U ratios (<0.1) suggest a metamorphic source.

before source tracing (McLennan et al., 1983; Feng and Kerrich, 1990; Roddaz et al., 2012).

Chemical Index of Alteration (CIA) is one of the important indexes to measure the chemical weathering degree of sediments (Nesbitt and Young, 1982; Shao et al., 2012; Huyan and Yao, 2022). The formula is: $\text{CIA} = [\text{Al}_2\text{O}_3 / (\text{Al}_2\text{O}_3 + \text{CaO}^* + \text{Na}_2\text{O} + \text{K}_2\text{O})] \times 100$. In the expression, the principal component refers to the mole fraction, where CaO^* is the molecular weight of CaO in the silicate part (McLennan, 1993a). Larger CIA values correspond to higher

degrees of chemical weathering (Fedo et al., 1995). In this study, the CIA values of the LR sediments are similar to those of the JSR sediments, with the range of 51.4–57.6, indicating incipient chemical weathering degree, which is comparable to the chemical weathering level of Quaternary aeolian sediments and river sediments in this area (CIA = 51.2–60.0, Xie et al., 2018a; Xie et al., 2018b; Zhao et al., 2023).

Because K-metasomatism may interfere with the determination of CIA values, the use of CIW (Chemical Index of Weathering, $\text{CIW} = [\text{Al}_2\text{O}_3 / (\text{Al}_2\text{O}_3 + \text{CaO}^* + \text{Na}_2\text{O})] \times 100$) can effectively avoid the migration of K element during diagenesis or metamorphism (Harnois, 1988). The CIW values of the LR and JSR sediments are 59.7–62.7 and 61.5–66.1, respectively, showing a low degree of chemical weathering. Plagioclase Index of Alteration (PIA) is also used for a correction for K-metasomatism (Fedo et al., 1995), and calculated as follows: $\text{PIA} = [(\text{Al}_2\text{O}_3 - \text{K}_2\text{O}) / (\text{Al}_2\text{O}_3 + \text{CaO}^* + \text{Na}_2\text{O} - \text{K}_2\text{O})] \times 100$. The PIA values (52.0–60.2) of the two rivers show low chemical weathering levels. In the A-CN-K compositional space constructed for this study (Fig. 9), the samples are plotted close to UCC and parallel to the A-CN line, indicating no effect of K-metasomatism and low levels of chemical weathering (Nesbitt and Young, 1984; Fedo et al., 1995).

Weathering Index of Parker (WIP = $[(2\text{Na}_2\text{O}/0.35) + (\text{MgO}/0.9) + (2\text{K}_2\text{O}/0.25) + (\text{CaO}^*/0.7)] \times 100$, Parker, 1970) is more sensitive to the accumulation of quartz and zircon caused by sedimentary cycle and sorting. The WIP values of the two rivers are similar but have little difference, ranging from 56.0 to 65.5, which indicates low levels of the chemical weathering. In addition, Rb/Sr ratio was also widely used to determine the degree of chemical weathering (Chen et al., 1999; Jin et al., 2006; Xu et al., 2010; Chang et al., 2013; An et al., 2018). The Rb/Sr ratios of the LR and JSR are 0.38 and 0.42, respectively, much lower than the PAAS values (Taylor and Bradley, 1985), indicating incipient degrees of chemical weathering (Wang et al., 2020).

In the process of chemical weathering, some immobile element references (e.g., Al and Ti) are usually selected to calculate the mass migration coefficient of each element (Nesbitt, 1979). In this study, the high contents of Al element in the sediments indicate no clear leaching of Al element (Supplementary Tables S1). Therefore, Al element is selected as the immobile element reference in this study to evaluate the relative loss or enrichment degree of elements in chemical weathering process by using the material balance coefficient (X_{change}). The formula for material balance coefficient is:

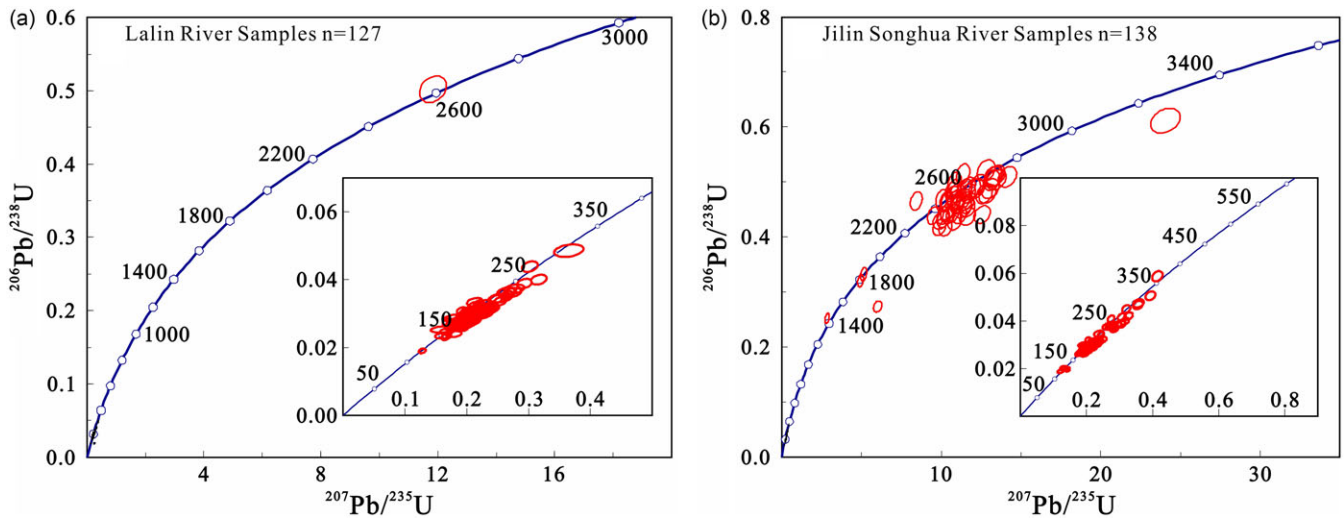


Figure 7. U-Pb Concordia diagrams (a-b) for the detrital zircon grains of the Lalin River and Jilin Songhua River sediments.

$$X_{\text{change}} = (X_{\text{ws}}/Y_{\text{ws}})/(X_{\text{pr}}/Y_{\text{pr}}) - 1$$

In the formula, X_{ws} and X_{pr} are the concentration of elements in the sample and UCC, respectively, and Y_{ws} and Y_{pr} are the concentration of immobile elements in the sample and UCC (i.e., Al), respectively. The results show a clear leaching of Mg and Ca, but no clear leaching of Na and K (Fig. 10). Cautions are that in the source rocks of the two rivers, the proportion of acid igneous rocks is the largest (Table 1), and the Mg content is relatively low. Therefore, the relative loss of Mg is due to the difference of source-rock types rather than chemical weathering.

In conclusion, both two river sediments are marked by incipient chemical weathering, thus indicating a weak effect of chemical weathering on the composition of the river sediments. It draws a conclusion that the geochemical composition of the two river sediments can be employed for the source-area tracing.

4. b. The influence of sedimentary recycling on the river sediments

The sorting and recycling of minerals during the transport and sedimentation processes of sediments will affect the material composition of river sediments, and even mask the provenance information from the parent rocks of source area (Condie, 1991; Cullers and Podkovyrov, 2000; Schneider et al., 2016). Therefore, it is necessary to evaluate the effect of sedimentary recycling on river sediments.

$\text{SiO}_2/\text{Al}_2\text{O}_3$ ratio is often used to evaluate sediment maturity, with a positive correlation with sediment maturity (El-Bialy, 2013; Armstrong-Altrin et al., 2015). In magmatic rocks, the variation range of this index is small, from about 3 in basic rocks (such as basalt) to about 5 in acidic rocks (such as granite and rhyolite) (Lemaitre, 1976; Roser et al., 1996). Therefore, a ratio greater than 5 or 6 indicates the maturity and sediment cycles, while a ratio greater than 7 indicates the strong maturity of sediments (Xie et al., 2019b). The mean values of $\text{SiO}_2/\text{Al}_2\text{O}_3$ in the LR and the JSR are 5.79 and 5.03, respectively, indicating low maturity.

The Index of Compositional Variability (ICV) is usually used to evaluate the maturity characteristics of sediments and distinguish the sedimentary recycling process (Cox et al., 1995; Cullers and Podkovyrov, 2000; Armstrong-Altrin et al., 2015;

Wang et al., 2015b; Perri et al., 2016; Huyan et al., 2021). The formula is: $\text{ICV} = (\text{CaO} + \text{K}_2\text{O} + \text{Na}_2\text{O} + \text{Fe}_2\text{O}_3 + \text{MgO} + \text{TiO}_2 + \text{MnO})/\text{Al}_2\text{O}_3$. In the formula, CaO represents the CaO in all components, and Fe_2O_3 represents the total iron content. $\text{ICV} > 1$ indicates a low maturity of sediments, the first deposition under tectonic activity, while $\text{ICV} < 1$ indicates a high maturity of sediments, the first cycle under high chemical weathering or strongly affected by recycling (Weaver, 1989; Cox et al., 1995; Tobia et al., 2019). The ICV values of the LR and the JSR are similar, with the mean values of 1.0 and 1.2, respectively, indicating their low maturities and/or low degree of recycling characteristics.

WIP, combined with CIA indicator, is more accurate to identify the degree of recycling (Fig. 11a) (Garzanti et al., 2013; Garzanti and Resentini, 2016). The CIA/WIP ratios of the LR and JSR sediments are less than 2, which proves their initial sedimentary cycling (Garzanti et al., 2013). In the CIA-WIP binary diagram (Fig. 11a), the sediments in this study are plotted along the trend line of chemical weathering of UCC, indicating a poor degree of sedimentary recycling. In mafic-felsic-weathering (Ohta and Arai, 2007) ternary diagram (Fig. 11b), the data points of the LR and JSR sediments are plotted along the igneous rock trend line, close to UCC and far away from the W vertex, indicating a low degree of weathering and a low sedimentary recycling (Ohta and Arai, 2007; Xie et al., 2019b; Li et al., 2023a).

Th/Sc-Zr/Sc binary diagram can well evaluate the potential effect of sedimentary processes (e.g., sorting and recycling) on sediments (McLennan et al., 1990; Xie et al., 2019b). Zr/Sc ratio commonly shows a clear increase but a far less increase of the Th/Sc ratio during multiple recycled processes (McLennan et al., 1990; McLennan et al., 1993b). In the Th/Sc-Zr/Sc binary diagram (Fig. 11c), the LR sediments array along zircon addition direction with a deviation from the magmatic composition trend line, whereas the JSR sediments are plotted close to the magmatic composition trend line slightly with zircon addition trend, indicating a minimal effect of sedimentary processes.

4. c. Control of the river sediments by source rocks

Source rocks are one of the most important factors affecting the composition of river sediments, which in turn indicates that the composition of river sediments also has a good response to

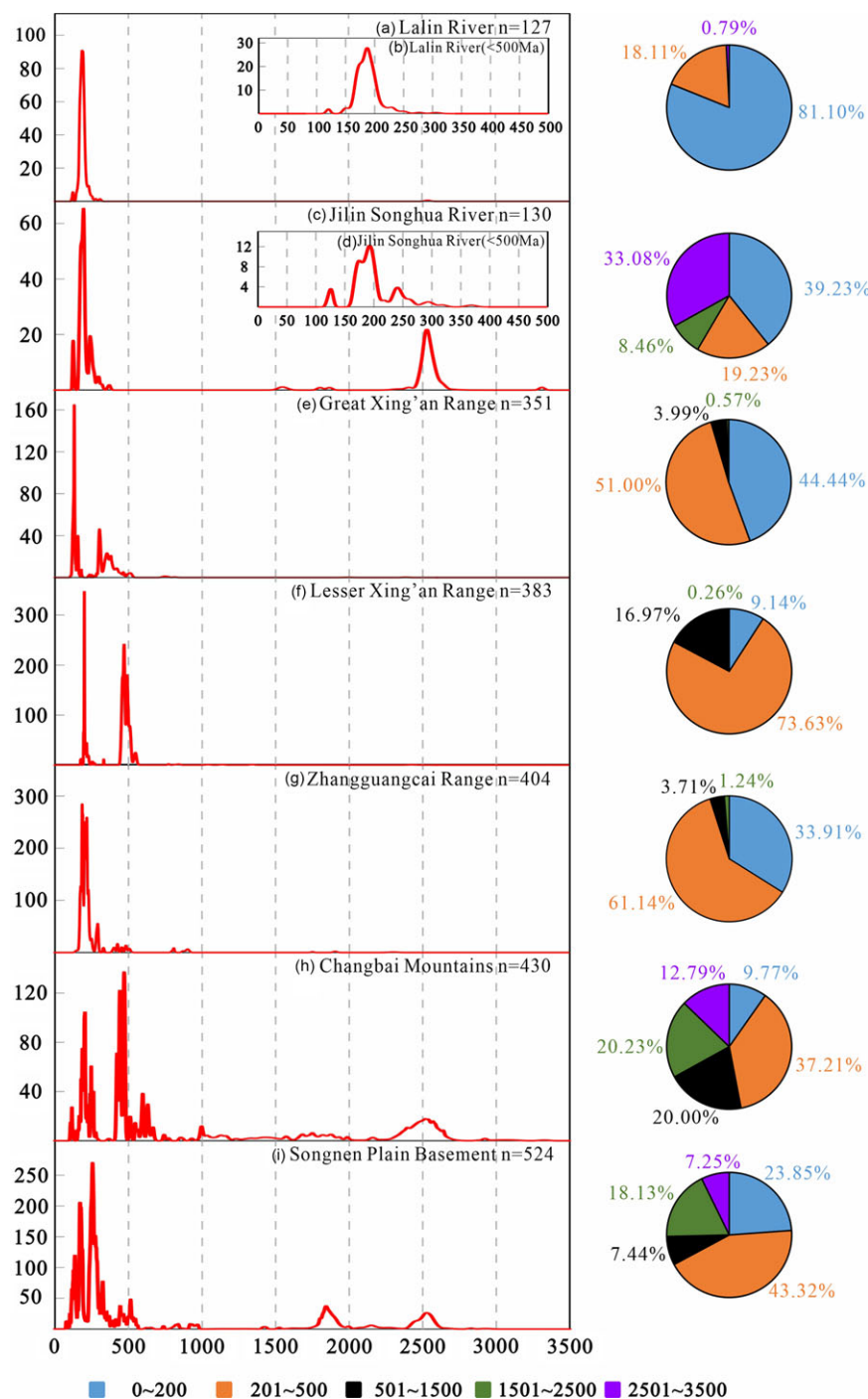


Figure 8. PDP plots for the detrital zircon ages of the two rivers. (a) the Lalin River in this study; (b) the Lalin River in this study (only containing less than 500 Ma); (c) the Jilin Songhua River in this study; (d) the Jilin Songhua River in this study (only containing less than 500 Ma); (e) igneous zircon ages in the Great Xing'an Range compiled from Wu et al., 2011; Liu et al., 2014; Zhang et al., 2015; Wang et al., 2018; Song et al., 2019; Wang and Yang, 2019; Chen et al., 2021; Jia et al., 2022; (f) igneous zircon ages in the the Lesser Xing'an Range compiled from Wu et al., 2011; Li et al., 2019; Wang et al., 2016a; (g) igneous zircon ages in the Zhangguangcai Range compiled from Wu et al., 2011; Xu et al., 2013; Wang et al., 2015c; (h) igneous zircon ages in the Changbai Mountains compiled from Wu et al., 2011; Wang et al., 2016b; Zhang et al., 2017; (i) igneous zircon ages in the Songnen Plain basement compiled from Wang et al., 2006; Li et al., 2012; Song et al., 2012; Jia et al., 2016; Huang et al., 2019; Zang et al., 2023.

sediment provenance properties and their tectonic settings (Gabo et al., 2009; Jian et al., 2013). In this section, we use mineralogy, elemental geochemistry and detrital zircon U-Pb dating to distinguish the types of parent rocks in the source area and explore the extent of their influence on the river sediments.

4. c.1. Change characteristics of heavy minerals

The LR and JSR sediments show the notable differences in some of the characteristic heavy minerals (Fig. 4), e.g., haematite-limonite, magnetic haematite, epidote, apatite, hornblende, magnetite, pyroxene and zircon. The different parent rocks in the source areas and later weathering and alteration are responsible for these

differences. Large areas of mafic rocks (e.g., basalts) are outcropped in the source area and course of the JSR (Fig. 2c), and they are depleted in zircon and are highly susceptible to weathering and alteration, thus resulting in more weathering-alteration minerals (e.g., haematite, limonite, magnetic haematite) occurring in the JSR sediments (Fig. 4). In addition, the formation of epidote is a result of the dynamic metamorphism of basic igneous rocks and/or the potassium-metasomatism of hornblende (Marmo, 1979). The large area of basalt outcrops in the source area of the JSR and the multiple tectonic movements in geological history (Liu et al., 2015; Qiao et al., 2016) have provided the high epidote content in the JSR.

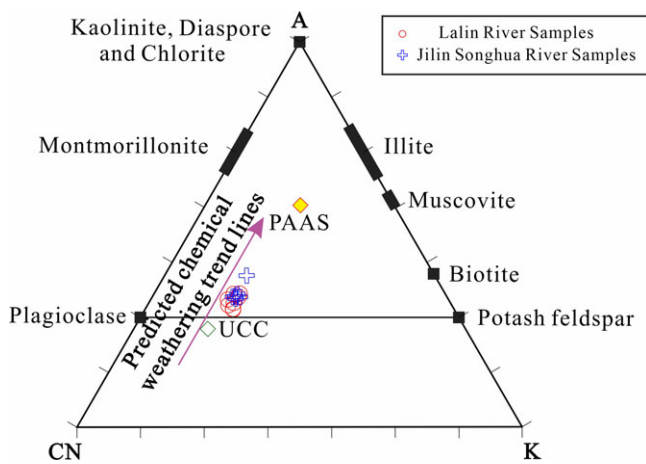


Figure 9. A-CN-K ($\text{Al}_2\text{O}_3\text{-CaO}^*+\text{Na}_2\text{O-K}_2\text{O}$) ternary diagram (in molecular proportion, after Nesbitt and Young, 1984), characterizing weathering trend of the Lalin River and Jilin Songhua River sediments. UCC and Post Archean Australian shale values are from Taylor and McLennan (1985).

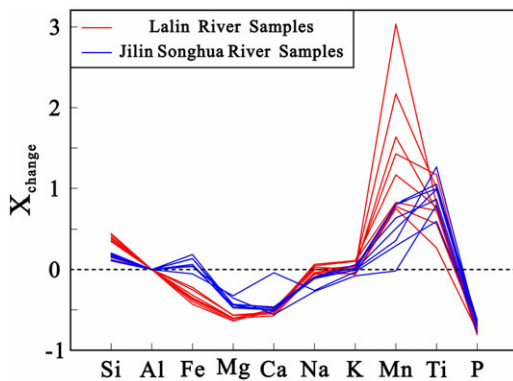


Figure 10. Bivariate plots showing relative depletion or enrichment of major elements relative to element Al reference.

Significantly, the marked differences in the heavy mineral composition can be observed in the different grain-sized fractions, most notably in hornblende and epidote (Fig. 4). More specifically, hornblende is clearly enriched in the coarse-sized fractions (especially 125–250 μm) compared to the <63 μm in the two rivers, indicating its grain size dependency being controlled by hydrodynamic sorting (Mange and Maurer, 1992). However, epidote presents the contrasting enrichment patterns in the two rivers, enrichment in <63 μm for the LR and in 125–250 μm for the JSR, which cannot be explained by mineral sorting. In addition to mineral sorting during sedimentary transportation, initial size of the heavy minerals in source areas also affects grain size dependency of heavy mineral composition. In this sense, more caution should be exercised when using heavy minerals for source tracing, as characterized by other observations (Zhang et al., 2020).

4. c.2. Change characteristics of Sr-Nd isotopes

Sr isotopes are subject to potential factors, e.g., chemical weathering, diagenesis and particle size effects during weathering, transport and deposition (Walter et al., 2000; Rao et al., 2006; Rao et al., 2011), thus providing less provenance information (Chen et al., 2007). However, Nd isotopes are very little affected by non-source factors (Jones et al., 1994; Grousset and Biscaye, 2005;

Rao et al., 2006; Chen et al., 2007; Asahara et al., 2012) and thus have been widely used as a powerful source tracer (Goldstein et al., 1984; Goldstein and Jacobsen, 1988; Aubert et al., 2002; Jiang et al., 2019).

The two river sediments share the similar Sr isotopic ratios, as also is the case for their similar degree of chemical weathering and sedimentary recycling, whereas Nd isotopic ratios distinguish well between the two river sediments, with significantly positive Nd isotopic ratios for the LR (Fig. 5). This observation once indicates the source-area dependency of Nd isotopic ratio. Notably, both the two river sediments show the significant variations of the $\epsilon_{\text{Nd}}(0)$ values, with an inter-sediment variation in the same river exceeding 2ϵ , which is well in excess of the threshold (1ϵ units) of experimental error (Xie et al., 2020). These findings indicate that Nd isotopic variations between sediments in the same river are essentially triggered by the sustained denudation and thus addition of different parent rocks in process of sediment transportation. This is an indication of the heterogeneity of the river sediments.

4. c.3. Change Characteristics of U-Pb ages in detrital zircons

The two river sediments are of the drastically different detrital zircon U-Pb age characteristics (Fig. 8), with a clear peak age at ~2.5 Ga for the JSR. The 100–400 Ma-aged zircons generally occur in the mountains surrounding the Songnen Plain, e.g., the Great Xing'an Range, the Lesser Xing'an Range, the Zhangguangcai Range and the Changbai Mountains, despite slightly different peak age. Accordingly, the two rivers have the similar age pattern at 100–400 Ma intervals, despite a few sub-peak ages in the JSR. The Precambrian detrital zircons only occur in the basement of the Songnen Plain and the northeastern NCC (Fig. 8), but almost lacking in the young orogenic belt (Great Xing'an Range, Lesser Xing'an Range and Zhangguangcai Range). The notable peak age of ~2.5 Ga in the JSR but not in the LR indicates the detrital contributions of the northeastern NCC to the JSR, as evidenced by the widely outcropped Neoproterozoic parent rocks (e.g., amphibolite, granulite, gneiss and granite, Fig. 2c) in the headwater. Accordingly, the lithological differences in the headwater area have led to significantly different detrital zircon U-Pb age patterns in the sediments of the two rivers.

Notably, the U-Pb age composition of the detrital zircons in the two rivers does not well match the exposed area ratios of different types of the source rocks in the basin (Fig. 8a-d and Table 1). This discordance can be attributed to the differences such as power and range of fluvial erosion, as well as zircon fertility in source areas.

4. c.4. Evaluation of immobile element ratios in identification of the parent-rock nature

Some immobile trace elements and their ratios are usually used to depict the parent-rock properties (felsic/mafic source) of sediments (Cullers et al., 1988; Condie and Wronkiewicz, 1990). For example, high-field strength elements La, Th, Zr and U are mainly enriched in acidic (felsic) parent rocks (Cullers, 1995), and transition elements Sc, Co, Cr and Ni are mainly enriched in basic (mafic) rocks (Feng and Kerrich, 1990). In the discrimination diagrams characterizing parent-rock nature with immobile elements in this study (Fig. 12), the two river sediments cluster together in the felsic source region, indicating their felsic parent rocks in origin. This is true for the LR sediments because their source area is lithologically dominated by late Triassic-Cretaceous granite and intermediate-acid igneous rocks (Fig. 2c). However, this is not the case for the JSR sediments. In the upstream area southeast of Jilin city, basalts are sporadically exposed in the

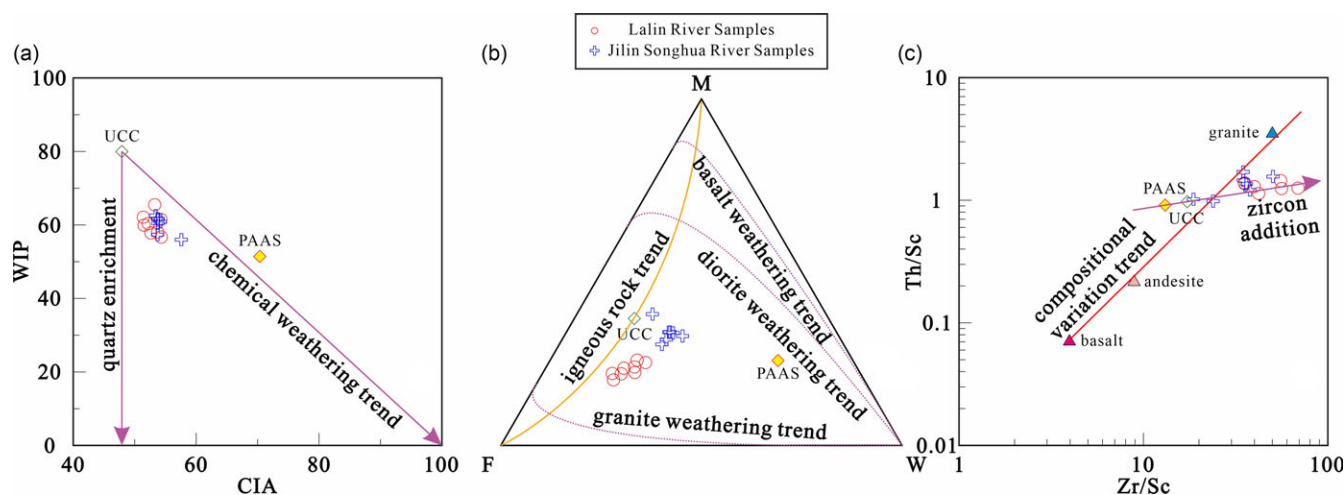


Figure 11. Discriminant diagrams for sedimentary recycling in the Lalin River and Jilin Songhua River sediments. (a) CIA vs. WIP plot distinguishing first-cycle and recycling sediments (after Garzanti et al., 2013). Because quartz dilution strongly affects WIP but not CIA, the CIA/WIP plot readily reveals quartz enrichment in sediments due to recycling sedimentation. The studied samples plot well below UCC weathering trend line, reflecting some degrees of sedimentary recycling; (b) The MFW (Mafic-Felsic-Weathering) plots, served as depicting tendency and intensity of weathering (after Ohta and Arai, 2007) as well as distinguishing first-cycle from recycling processes (after Ohta, 2008). The studied sediments plot along a trend close to igneous rock compositional trend and to the F-W line, but far away from W apex, suggesting low degree of chemical weathering and dominant felsic and minor intermediate rocks in their primitive source areas. In addition, the weathering trend of these sediments does not extend towards the W vertex but instead, arrays along igneous rock compositional trend towards the M vertex, indicating that they cannot be represented by the weathering of the igneous rocks, i.e. they are of nature of recycling sedimentation; (c) Th/Sc v. Zr/Sc bivariate plot (after McLennan et al., 1993b) for the sediments of the Lalin River and the Jilin Songhua River, identifying whether the sediments are derived from recycled sedimentation. UCC and Post Archean Australian shale values are from Taylor and McLennan (1985). $M = \exp.(-0.395 \cdot \ln(\text{SiO}_2) + 0.206 \cdot \ln(\text{TiO}_2) - 0.316 \cdot \ln(\text{Al}_2\text{O}_3) + 0.16 \cdot \ln(\text{Fe}_2\text{O}_3) + 0.246 \cdot \ln(\text{MgO}) + 0.368 \cdot \ln(\text{CaO}) + 0.073 \cdot \ln(\text{Na}_2\text{O}) - 0.342 \cdot \ln(\text{K}_2\text{O}) + 2.266)$. $F = \exp.(0.191 \cdot \ln(\text{SiO}_2) - 0.397 \cdot \ln(\text{TiO}_2) + 0.02 \cdot \ln(\text{Al}_2\text{O}_3) - 0.375 \cdot \ln(\text{Fe}_2\text{O}_3) - 0.243 \cdot \ln(\text{MgO}) + 0.079 \cdot \ln(\text{CaO}) + 0.392 \cdot \ln(\text{Na}_2\text{O}) + 0.333 \cdot \ln(\text{K}_2\text{O}) - 0.892)$. $W = \exp.(0.203 \cdot \ln(\text{SiO}_2) + 0.191 \cdot \ln(\text{TiO}_2) + 0.296 \cdot \ln(\text{Al}_2\text{O}_3) + 0.215 \cdot \ln(\text{Fe}_2\text{O}_3) - 0.002 \cdot \ln(\text{MgO}) - 0.448 \cdot \ln(\text{CaO}) - 0.464 \cdot \ln(\text{Na}_2\text{O}) + 0.008 \cdot \ln(\text{K}_2\text{O}) - 1.374)$.

intermediate-acid igneous rocks, especially in the headwater near Fusong county, where basalts are widely exposed, whereas the downstream area northwest of Jilin city is covered by the sporadic intermediate-acid igneous rocks and widely exposed Quaternary sediments. The basalt information occurring in the upper reaches of the JSR is not reflected in the commonly used discrimination diagrams of parent-rock natures (Fig. 12), and we speculate that these basalt records are likely to have been masked by the records from the widely outcropped intermediate-acid igneous rocks. In this sense, the employment of immobile element ratios to the parent-rock nature identification needs to be treated with caution.

4. d. Implications for regional tectonic and magmatic activities in the Southeastern Songnen Plain

The river sediments obtain the attention of a wide range of scholars due to their records of information about source-area tectonic and magmatic activities using detrital zircon ages (Jie et al., 2007; Han et al., 2017; Liang et al., 2018; Li et al., 2023b). The headwater regions of the LR and the JSR are tectonically located at the eastern part of the CAO and the northeastern end of the NCC, respectively. Accordingly, the study area involves the geological evolution history of tectonic and magmatic events, e.g., the formation of the Precambrian NCC, the closure of the Paleo-Early Mesozoic Asian Ocean and the subduction and retreat of the Paleo-Pacific plate in the Mesozoic.

It is generally accepted that peak ages of detrital zircons correspond to a certain scale of tectonic-magmatic events that occurred in the source area during this period (Kong et al., 2022), as different from biased geochemical methods (Rudnick and Gao, 2003). In this study, the main age peaks of 119–306 Ma in the LR (Fig. 8a, b) as well as 120–368 Ma and 2480–2667 Ma in the JSR (Fig. 8c-f) are the comprehensive responses to the

multi-stage tectono-magmatic events in the different periods in the study area.

The early Precambrian period was the rapid growth stage of the Earth's continents, and 70% of the continental crust was formed during the Archean period (Condie, 1994, 1998). The NCC, one of the oldest cratons in the world, underwent complex multi-stage tectonic evolution (Kusky et al., 2007; Wan et al., 2008, 2015, 2017), with age back as far as 4.0–3.8 Ga (Wan et al., 2001, 2020, 2021a, 2021b). Paleoproterozoic-early Neoproterozoic (3.6–2.6 Ga) continental growth was dominated by plate floor support or mantle overturning activities, which caused large-scale magmatic activity and metamorphism, and Trondhjemite, Tonalite and Granodiorite (TTG) rocks began to be found at many sites in NCC (Wan et al., 2012, 2017). However, pre-Mesoproterozoic (2.8 Ga) mainly existed in the eastern, southern and central landmasses divided by Wan et al. (2015). The three main tectono-magmatic events occurred in the NCC since the Neoproterozoic, i.e., extensive crustal accretion at 2.9–2.7 Ga, crustal growth and cratonisation marked by numerous tectonic and metamorphic-magmatic events at 2.5 Ga, and the final formation of the craton at 1.8 Ga (Shen et al., 1999; Zhai and Bian, 2000; Zhao et al., 2001, 2005; Kusky and Li, 2003; Kröner et al., 2005; Kusky et al., 2007; Geng et al., 2010; Zhai, 2010; Geng et al., 2012; Diwu et al., 2012; Hu et al., 2013; Wang et al., 2023). Among them, the most important magmatic-thermal events occurred at 2.5 Ga (Kröner et al., 2005; Shen et al., 2005; Zhao et al., 2005; Diwu et al., 2012), as is the specificity of NCC different from other ancient continents (Windley, 1995; Liu et al., 2009). The upper reaches of the JSR, e.g., the areas near Huadian, Jingyu and Fusong county, are lithologically marked by the widely outcropped Neoproterozoic amphibolite, granulite, gneiss and granite (Fig. 2c), which, combined with the prominent peak age at 2.5–2.6 Ga of the detrital zircons in the JSR (Fig. 8), confirms the strong tectono-thermal events in that period in the

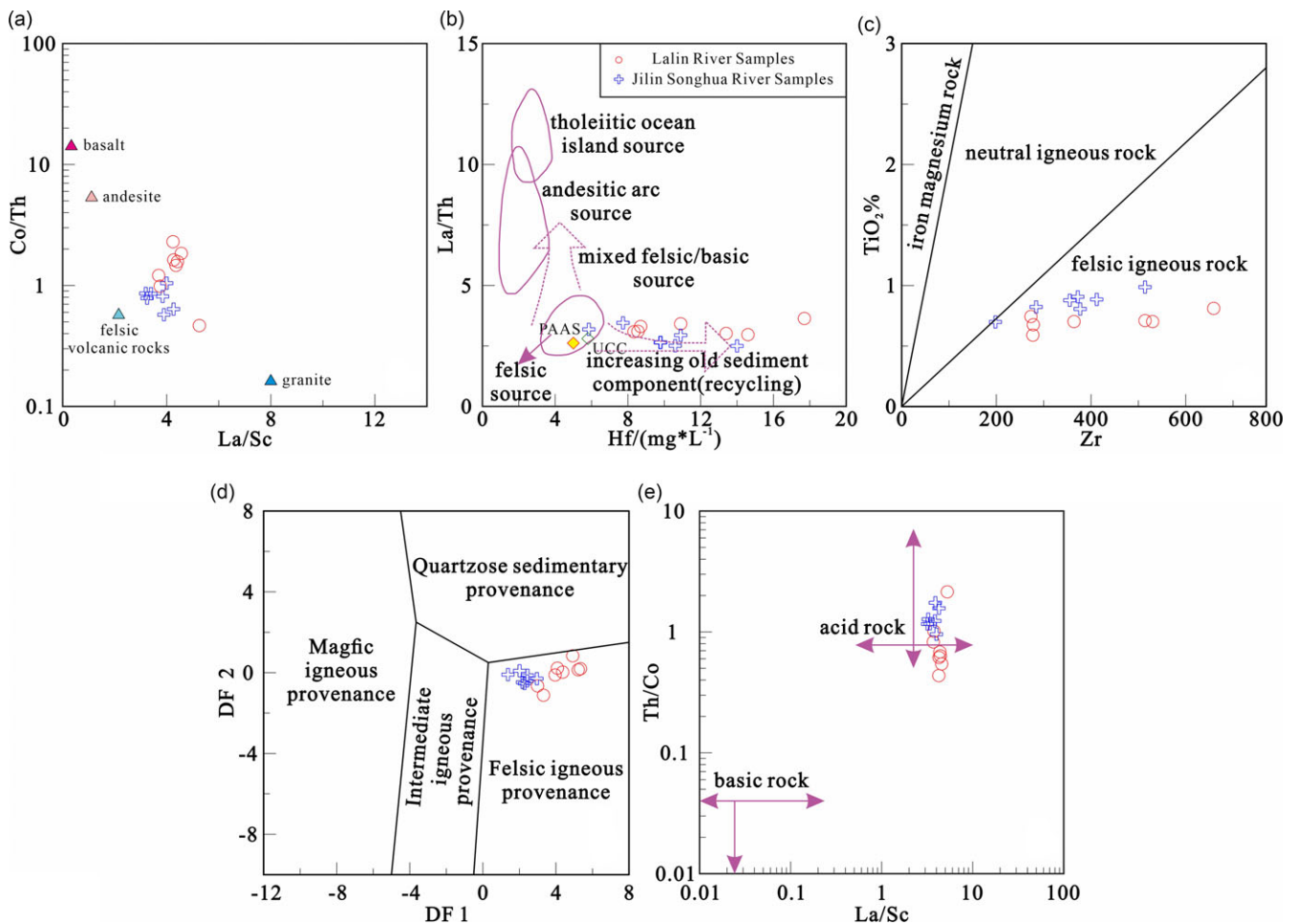


Figure 12. Discrimination diagrams illustrating source-rock nature with immobile trace elements for the Lalin River and Jilin Songhua River sediments. (a) Co/Th vs. La/Sc plot after Gu (1994); (b) La/Th–Hf diagram after Floyd and Leveridge (1987); (c) Discriminant diagram of TiO₂%–Zr; (d) Provenance discrimination function diagram (after Roser and Korsch, 1986). The studied samples plot across felsic igneous and quartzose sedimentary provenance fields, suggesting characteristics of sediment recycling and felsic components in their ultimate source area. (e) Discriminant diagram of Th/Co–La/Sc. DF1 = 30.638 × TiO₂/Al₂O₃ – 12.541 × Fe₂O₃/Al₂O₃ + 7.329 × MgO/Al₂O₃ + 12.031 × Na₂O/Al₂O₃ + 35.42 × K₂O/Al₂O₃ – 6.382. DF2 = 56.500 × TiO₂/Al₂O₃ – 10.879 × Fe₂O₃/Al₂O₃ + 30.875 × MgO/Al₂O₃ – 5.404 × Na₂O/Al₂O₃ + 11.112 × K₂O/Al₂O₃ – 3.89.

northeastern NCC. This result also corroborates that 2.5–2.6 Ga event is one of the strongest tectono-magmatic events in the NCC (Kröner et al., 2005; Zhao et al., 2005; Liu et al., 2009; Diwu et al., 2012; Wang et al., 2023), which induced an important crustal growth and thus its cratonisation. Notably, the 2.9–2.7 Ga and 1.8 Ga events are not documented in the northeastern NCC.

The formation of the Solonker-Xar Moron-Changchun suture zone represents the formation of the southern edge of the CAOB and the final closure of the Paleo-Asian Ocean, closely related to the collision between the NCC and the Siberian Craton (Xu et al., 2013; Wang et al., 2015d). The timing of the final closure of the Paleo-Asian Ocean has aroused wide controversy (Xiao et al., 2003, 2009; Windley et al., 2007; Ren et al., 2023; Wang et al., 2024), with variable ages at Carboniferous (Chen et al., 2022), Lower Permian (Li, 2006), Upper Permian–Lower Triassic (Sun et al., 2005; Li et al., 2007; Cao et al., 2013), Lower Triassic (Wu et al., 2007a) and Middle Triassic (Wang et al., 2024). We conclude, therefore, that the minor detrital zircon peak age at Carboniferous–Triassic (300–230 Ma, Fig. 8) in the JSR responds to the closure event of the Paleo-Asian Ocean. It is universally recognized that the Paleo-Pacific plate began to subduct westward beneath the Eurasian continent at the Jurassic period (Wu et al., 2007b; Tang et al., 2018a;

Li et al., 2020; Li et al., 2024) and rollback eastward at the Early Cretaceous period (Tang et al., 2018b; Ma and Xu, 2021). This subduction and rollback triggered the large-scale magmatic activity in the late Mesozoic in northeast China, which made the Mesozoic igneous rocks widely developed in the upper reaches of the LR and the JSR (Fig. 2c). Therefore, the prominent peak ages of detrital zircons in the two rivers, ranging from 200 to 150 Ma (Fig. 8) are a good response to the subduction event of the ancient Pacific Plate. Compared to very poor age group at ~120 Ma in the LR (Fig. 8), slightly pronounced peak age at ~120 Ma in the JSR documents the rollback event of the Paleo-Pacific plate. The notable difference between detrital zircon ages and resultant records of regional tectono-magmatic events for the two rivers is determined by the different parent rocks in the source areas.

5. Conclusions

The sediments from the LR and the JSR are compared in terms of geochemistry (element and Sr–Nd isotopic composition), heavy mineral and detrital zircon U–Pb dating. The major conclusions are drawn as follows:

- (1) The two rivers have similar geochemical compositions (such as elements and Sr isotopes) as well as weak chemical weathering and cycling characteristics, indicating that the geochemical composition of the river sediments is mainly controlled by climate rather than provenance.
- (2) Significant differences exist in the detrital zircon U-Pb ages, Nd isotopic ratios and to a certain extent heavy mineral composition for the two rivers, indicating source control. The heterogeneity of the river sediments is indicated by the significantly variable Nd isotope ratios. The information from basic parent rocks could not be identified by element geochemical methods due to the dilution of widely exposed acidic rocks.
- (3) The clear U-Pb multi-peak ages of the detrital zircons from the JSR record the crust growth and cratonization of the NCC during the 2.5 Ga period. The minor peak age of the Carboniferous-Triassic (300-230 Ma) detrital zircons in the JSR responds to the Paleo-Asian Ocean closure event. The prominent age of the detrital zircons in the two rivers is 200-150 Ma, which is a good response to the subduction event of the Paleo-Pacific plate. Compared with the very poor age group of ~120 Ma in the LR, the slight peak age of ~120 Ma in the JSR records the rollback event of the Paleo-Pacific plate. The significant differences in the detrital zircon ages and regional tectono-magmatic records between the two rivers are determined by the different parent rocks in the source areas.

Supplementary material. The supplementary material for this article can be found <https://doi.org/10.1017/S0016756824000517>

Acknowledgements. The geochemical analysis was supported by the State Key Laboratory of Geological Processes and Mineral Resources, China University of Geosciences (Wuhan), heavy minerals were detected by Chengxin Geology Company, Langfang, Hebei, and the U-Pb dating analysis of detrital zircons was measured by Ms. Xiaoli Yan, Lanzhou University. Thanks to Fengzhan Guo and Xiaoyu Han for their participation in the discussion of the paper writing.

Financial support. This study was financially supported by the National Natural Science Foundation of China (Grant: 42171006 and 41871013).

Competing interests. The authors declared that they have no conflicts of interest in this work. We declare that we do not have any commercial or associative interest that represents a conflict of interest in connection with the work submitted.

Reference

- Algeo TJ and Maynard JB, (2004) Trace-element behavior and redox facies in core shales of Upper Pennsylvanian Kansas-type cyclothems. *Chemical Geology* **206**(3-4), 289–318.
- An FY, Lai ZP, Liu XJ, Fan QS and Wei HC, (2018) Abnormal Rb/Sr ratio in lacustrine sediments of Qaidam Basin, NE Qinghai-Tibetan Plateau: A significant role of aeolian dust input. *Quaternary International* **469** (Part A), 44–57.
- Andersen T, (2002) Correction of common lead in U–Pb analyses that do not report ²⁰⁴Pb. *Chemical Geology* **192**(1–2), 59–79.
- Arató R, Obbágy G, Dunkl I, Józsa S, Lünsdorf K, Szepesi J, Benkó Z, Molnár K and Eynatten HV, (2021) Multi-method comparison of modern river sediments in the Pannonian Basin System – A key step towards understanding the provenance of sedimentary basin-fill. *Global and Planetary Change* **199**, 103446.
- Armstrong-Altrin JS, Nagarajan R, Balaran V and Natalhy-Pineda O, (2015) Petrography and geochemistry of sands from the Chachalacas and Veracruz beach areas, western Gulf of Mexico, Mexico: Constraints on provenance and tectonic setting. *Journal of South American Earth Sciences* **64**(Part 1), 199–216.
- Asahara Y, Takeuchi F, Nagashima K, Harada N, Yamamoto K, Oguri K and Tadao O, (2012) Provenance of terrigenous detritus of the surface sediments in the Bering and Chukchi Seas as derived from Sr and Nd isotopes: Implications for recent climate change in the Arctic regions. *Deep-Sea Research Part II: Topical Studies in Oceanography* **61-64**, 155–71.
- Aubert D, Probst A, Stille P, Stille P and Viville D, (2002) Evidence of hydrological control of Sr behavior in stream water (Strengbach catchment, Vosges mountains, France). *Applied Geochemistry* **17**(3), 285–300.
- Bao C, Chen YL and Li DP, (2013) Zircon U-Pb age, Hf isotope composition and geological significance of detrital sediments from the floodplain of Xilamulun River, Inner Mongolia. *Acta Petrologica Sinica*, **29**(9), 3159–3172 (in Chinese with English Abstract).
- Biscaye PE, Grousset FE, Revel M, Van der Gaas S, Zielins GA, Kukla G, (1997) Asian provenance of glacial dust (stage 2) in the Greenland Ice Sheet Project 2 Ice Core, Summit, Greenland. *Journal of Geophysical Research: Oceans* **102**(C12), 26765–81.
- Cao HH, Xu, WL, Pei FP, Wang ZW, Wang F and Wang ZJ, (2013) Zircon U–Pb geochronology and petrogenesis of the Late Paleozoic–Early Mesozoic intrusive rocks in the eastern segment of the northern margin of the North China Block. *Lithos* **170-171**, 191–207.
- Cao L, Liu JG, Shi XF, Wei H and Zhong C, (2019) Source-to-sink processes of fluvial sediments in the northern South China Sea: Constraints from river sediments in the coastal region of South China. *Journal of Asian Earth Sciences* **2019** (185), 104020.
- Carter SC, Griffith EM, Clift PD, Scher HD and Dellapenna TM, (2020) Clay-fraction strontium and neodymium isotopes in the Indus Fan: implications for sediment transport and provenance. *Geological Magazine* **157**(6), 879–94.
- Chang H, An ZS, Wu F, Jin ZD, Liu WG and Song YG, (2013) A Rb/Sr record of the weathering response to environmental changes in westerly winds across the Tarim Basin in the late Miocene to the early Pleistocene. *Palaeogeography Palaeoclimatology Palaeoecology* **386**(6), 364–73.
- Chen J, An ZS and Head J, (1999) Variation of Rb/Sr Ratios in the Loess-Paleosol Sequences of Central China during the Last 130,000 Years and Their Implications for Monsoon Paleoclimatology. *Quaternary Research* **51**, 215–19.
- Chen J, Li GJ, Yang JD, Rao WB, Lu HY, Balsam W, Sun YB and Ji JF, (2007) Nd and Sr isotopic characteristics of Chinese deserts: Implications for the provenances of Asian dust. *Geochimica et Cosmochimica Acta* **71**(15), 3904–14.
- Chen R, Wang F, Li Z, Evans NJ and Chen HD, (2022) Detrital zircon geochronology of the Permian Lower Shihezi Formation, northern Ordos Basin, China: time constraints for closing of the Palaeo-Asian Ocean. *Geological Magazine* **159**(9), 1601–20.
- Chen ZG, Li YS, Yu XF, Wang Y, Zhen SM and Gong FY, (2021) Characterization of the Xiaokelehe granite porphyry in the Northern Great Xing'an Range. *Earth Science Frontiers* **28**(4), 267–82 (in Chinese with English abstract).
- Chi GX, Liu BL, Hu K, Yang J and He BC, (2021) Geochemical composition of sediments in the Liao River Estuary and implications for provenance and weathering. *Regional Studies in Marine Science* **45**, 101833.
- Clift PD, Wan S and Blusztajn J, (2014) Reconstructing chemical weathering, physical erosion and monsoon intensity since 25 Ma in the northern South China Sea: A review of competing proxies. *Earth-Science Reviews* **130**, 86–102.
- Condie KC, (1991) Another look at rare earth elements in shales. *Geochimica et Cosmochimica Acta* **55**, 2527–31.
- Condie KC, (1994) Greenstones through time. In: *Archean Crustal Evolution* (ed. Condie K C) . Amsterdam: Elsevier Publisher, 85–120.
- Condie KC, (1998) Episodic continental growth and supercontinents: A mantle avalanche connection? *Earth and Planetary Science Letters* **163** (1-4), 97–108.
- Condie KC and Wronkiewicz DJ, (1990) The Cr/Th ratio in Precambrian pelites from the Kaapvaal Craton as an index of craton evolution. *Earth and Planetary Science Letters* **97**(3), 256–67.
- Corfu F, Hanchar JM, Hoskin PWO and Kinny P, (2003) Atlas of Zircon Textures. *Reviews in Mineralogy and Geochemistry* **53**(1), 469–500.

- Cox R, Lowe DR and Cullers RL**, (1995) The influence of sediment recycling and basement composition on evolution of mudrock chemistry in the southwestern United States. *Geochimica et Cosmochimica Acta* **59**(14), 2919–40.
- Cullers RL**, (1995) The controls on the major- and trace-element evolution of shales, siltstones and sandstones of Ordovician to tertiary age in the Wet Mountains region, Colorado, U.S.A. *Chemical Geology* **123**(1), 107–31.
- Cullers RL, Basu A and Suttner LJ**, (1988) Geochemical signature of provenance in sand-size material in soils and stream sediments near the Tobacco Root batholith, Montana, U.S.A. *Chemical Geology* **70**(4), 335–48.
- Cullers RL and Podkovyrov VN**, (2000) Geochemistry of the Mesoproterozoic Lakhanda shales in southeastern Yakutia, Russia: implications for mineralogical and provenance control, and recycling. *Precambrian Research* **104**(1), 77–93.
- Ding ZL, Sun JM, Yang SL and Liu TS**, (2001) Geochemistry of the Pliocene red clay formation in the Chinese Loess Plateau and implications for its origin, source provenance and paleoclimate change. *Geochimica et Cosmochimica Acta* **65**(6), 901–13.
- Diwu CY, Sun Y and Wang Q**, (2012) The crustal growth and evolution of North China Craton: Revealed by Hf isotopes in detrital zircons from modern rivers. *Acta Petrologica Sinica* **28**(11), 3520–30 (in Chinese with English abstract).
- El-Bialy MZ**, (2013) Geochemistry of the Neoproterozoic metasediments of Malhaq and Um Zariq formations, Kid metamorphic complex, Sinai, Egypt: Implications for source-area weathering, provenance, recycling, and depositional tectonic setting. *Lithos* **175**(8), 68–85.
- Fedo CM, Nesbitt HW and Young GM**, (1995) Unraveling the effects of potassium metasomatism in sedimentary rocks and paleosols, with implications for paleoweathering conditions and provenance. *Geology* **23**(10), 921–24.
- Feng R and Kerrich R**, (1990) Geochemistry of fine-grained clastic sediments in the Archean Abitibi greenstone belt, Canada: Implications for provenance and tectonic setting. *Geochimica et Cosmochimica Acta* **54**(4), 1061–81.
- Floyd PA and Leveridge BE** (1987) Tectonic environment of the Devonian Gramscatho basin, south Cornwall: framework mode and geochemical evidence from turbiditic sandstones. *Journal of the Geological Society, London* **144**, 531–42.
- Gabo JAS, Dimalanta CB, Asio MGS, Queaño KL, Yumul Jr GP, Imai A**, (2009) Geology and geochemistry of the clastic sequences from Northwestern Panay (Philippines): Implications for provenance and geotectonic setting. *Tectonophysics* **479**(1–2), 111–19.
- Gao JY, Gao JY, Cui YC, Sun LY, Han CP, Liu ZX, Huang YM, Dong Y, Pang LJ**, (1993). *Yushu County Annals*. Jilin Literature and History Press, 1–1057 (in Chinese).
- Gao L and Li GH**, (2011) Analysis of hydrological characteristics of the Second Songhua River. *Science and Technology Innovation Herald*, (35), 125–126 (in Chinese).
- Garzanti E, Padoan M, Andò S, Resentini AT, Vezzoli G and Lustrino M**, (2013) Weathering and relative durability of detrital minerals in equatorial climate: Sand petrology and geochemistry in the east African rift. *The Journal of Geology* **121**(6), 547–80.
- Garzanti E and Resentini A**, (2016) Provenance control on chemical indices of weathering (Taiwan river sands). *Sedimentary Geology* **336**, 81–95.
- Geng YS, Du LL and Ren LD**, (2012) Growth and reworking of the early Precambrian continental crust in the North China Craton: Constraints from zircon Hf isotopes. *Gondwana Research* **21**(2–3), 517–29.
- Geng YS, Shen QH and Ren LD**, (2010) Late Neoproterozoic to Early Paleoproterozoic magmatic events and tectonothermal systems in North China Craton. *Acta Petrologica Sinica*, **26**(7), 1945–66 (in Chinese with English abstract).
- Goldstein SL and Jacobsen SB**, (1988) Nd and Sr isotopic systematics of river water suspended material: implications for crustal evolution. *Earth and Planetary Science Letters* **87**, 249–65.
- Goldstein SL, O'Nions RK and Hamilton PJ**, (1984) A Sm-Nd isotopic study of atmospheric dusts and particulates from major river systems. *Earth and Planetary Science Letters* **70**(2), 221–36.
- Grousset FE and Biscaye PE**, (2005) Tracing dust sources and transport patterns using Sr, Nd and Pb isotopes. *Chemical Geology* **222**(3), 149–67.
- Gu XX**, 1994. Geochemical characteristics of the Triassic Tethys-turbidites in northwestern Sichuan, China: implications for provenance and interpretation of the tectonic setting. *Geochimica et Cosmochimica Acta* **58** (21), 4615–31.
- Guo P, Xu WL, Yu JJ, Wang F, Tang J and Li Y**, (2015) Geochronology and geochemistry of Late Triassic bimodal igneous rocks at the eastern margin of the Songnen–Zhangguangcai Range Massif, Northeast China: petrogenesis and tectonic implications. *International Geology Review* **58** (2), 196–215.
- Han PY, Guo JL, Chen K., Huang H, Zong KQ, Liu YS, Hu ZC and Gao S**, (2017) Widespread Neoproterozoic (~2.7–2.6 Ga) magmatism of the Yangtze craton, South China, as revealed by modern river detrital zircons. *Gondwana Research* **42**, 1–12.
- Hanchar JM and Miller CF**, (1993) Zircon zonation patterns as revealed by cathodoluminescence and backscattered electron images: Implications for interpretation of complex crustal histories. *Chemical Geology* **110**, 1–13.
- Harnois L**, (1988) The CIW index: A new chemical index of weathering. *Sedimentary Geology* **55**(3–4), 319–22.
- Heilongjiang Bureau of Geology and Mineral Resources (HBGMR)**, (1993) Regional Geology of Heilongjiang Province (in Chinese with English abstract). Geological Publishing House, Beijing, 734 pp.
- Hofer G, Wagneich M and Neuhuber, S**, (2013) Geochemistry of fine-grained sediments of the upper Cretaceous to Paleogene Gosau Group (Austria, Slovakia): Implications for paleoenvironmental and provenance studies. *Geoscience Frontiers* **4**(4), 449–68.
- Horn S and Schmincke HU**, (2000) Volatile emission during the eruption of Baitoushan Volcano (China/North Korea) ca. 969 AD. *Bulletin of Volcanology* **61**(8), 537–55.
- Hu B, Zhai MG, Peng P, Liu F, Diwu CR, Wang HZ and Zhang HD**, (2013) Late Paleoproterozoic to Neoproterozoic geological events of the North China Craton: evidences from LA-ICP-MS U-Pb geochronology of detrital zircons from the Cambrian and Jurassic sedimentary rocks in Western Hills of Beijing. *Acta Petrologica Sinica* **29**(7), 2508–36 (in Chinese with English abstract).
- Huang QH, Zhu GT, Wang H and Cheng HG**, (2019) Zircon U-Pb age of the basement rocks and its geological significances in Paleo-Central Uplift Belt of Songliao Basin. *Petroleum Geology and Oilfield Development in Daqing* **38**(3), 1–7 (in Chinese with English abstract).
- Huyan YY and Yao WS**, 2022. Geochemical comparisons of weathering, provenance and tectonics in the fluvial sediments from Yarlung Zangbo to Brahmaputra River. *Catena* **210**, 105944.
- Huyan YY, Yao WS and Xie XJ**, (2021) Provenance, source weathering, and tectonics of the Yarlung Zangbo River overbank sediments in Tibetan Plateau, China, using major, trace, and rare earth elements. *Geological Journal* **57**(1), 37–51.
- Huyan YY, Zhang BM, Wang XQ, Lu YX and Liu FT**, (2023) Geochemistry of the Lancang River (Upper Mekong River) overbank sediments: Implications for provenance, weathering and sedimentary characteristics. *Applied Geochemistry* **156**, 105747.
- Inner Mongolian Bureau of Geology and Mineral Resources (IMBGMR)**, (1992) Regional Geology of Inner Mongolia (in Chinese with English abstract). Geological Publishing House, Beijing, 725 pp.
- Jahn BM, Gallet S and Han J**, (2001) Geochemistry of the Xining, Xifeng and Jixian sections, Loess Plateau of China: eolian dust provenance and paleosol evolution during the last 140 ka. *Chemical Geology* **178**, 71–94.
- Jahn BM, Wu FY and Chen B**, (2000) Massive granitoid generation in Central Asia: Nd isotope evidence and implication for continental growth in the Phanerozoic. *Episodes* **23**, 2.
- Jia WX, Jiang QG, Wang DY and Gao W**, (2016) Captured zircon U-Pb ages in the mafic dike and constraints of the magmatic events in the basement of southern Songliao Basin. *Acta Petrologica Sinica* **32**(9), 2881–88 (in Chinese with English abstract).
- Jia X, Ren JG, Xu WT, Ma HC, Zhang C and Shi GM**, (2022) Zircon U-Pb dating of Late Paleozoic alkali-feldspar granite in Duobaoshan, Great

- Xing'an Range: constrains on collision and assembly time of Xing'an and Songnen Blocks. *Geology in China* **49**(2), 586–600 (in Chinese with English abstract).
- Jian X, Guan P, Zhang W and Feng F**, (2013) Geochemistry of Mesozoic and Cenozoic sediments in the northern Qaidam basin, northeastern Tibetan Plateau: Implications for provenance and weathering *Chemical Geology* **360–361**, 74–88.
- Jiang FQ, Xiong ZF, Frank M, Yin XB and Li AC**, (2019) The evolution and control of detrital sediment provenance in the middle and northern Okinawa Trough since the last deglaciation: Evidence from Sr and Nd isotopes. *Palaeogeography, Palaeoclimatology, Palaeoecology* **522**, 1–11.
- Jie Y, Gao S, Yuan HL, Gong HJ, Zhang H and Xie SW**, (2007) Detrital zircon ages of Hanjiang River: constraints on evolution of Northern Yangtze Craton, South China. *Journal of China University of Geosciences* **18**(3), 210–22.
- Jilin Bureau of Geology and Mineral Resources (JBGMR)**, (1988) Regional Geology of Jilin Province (in Chinese with English abstract) Geological Publishing House, Beijing, 698 pp.
- Jin ZD, Cao JJ, Wu JL and Wang SM**, (2006) A Rb/Sr record of catchment weathering response to Holocene climate change in Inner Mongolia. *Earth Surface Processes and Landforms* **31**(3), 285–91.
- Jones CE, Halliday AN, Rea DK and Owen RM**, (1994) Neodymium isotopic variations in North Pacific modern silicate sediment and the insignificance of detrital REE contributions to seawater. *Earth and Planetary Science Letters* **127**(1), 55–66.
- Jones CL, Orovan EA, Meffre S, Thompson J, Belousova EA, Cracknell MJ, Everard J, Bottrill R, Bodorkos S and Cooke, DR**, (2022) Zircon O and Lu-Hf isotope evidence of mantle and supracrustal origins of Tasmanian Devonian granites. *Gondwana Research* **110**, 1–12.
- Kang CG, Li CA, Wang JT and Shao L**, (2009) Heavy minerals characteristics of sediments in Jiangnan Plain and its indication to the forming of the three gorges. *Earth Science—Journal of China University of Geosciences* **34**(3), 419–27 (in Chinese with English Abstract).
- Kong LY, Guo P, Wan J, Liu CX, Wang J and Chen C**, (2022) Detrital zircon U-Pb geochronology and Hf isotopes of mesoproterozoic metasedimentary rocks in Dabie Orogen and its geological significance. *Earth Science* **47**(4), 1333–1348 (in Chinese with English abstract).
- Kröner A, Wilde SA, O'Brien PJ, Li JH, Passchier CW, Walte NP and Liu DY**, (2005) Field Relationships, Geochemistry, Zircon Ages and Evolution of a Late Archaean to Palaeoproterozoic Lower Crustal Section in the Hengshan Terrain of Northern China. *Acta Geologica Sinica*, **79**(5), 605–32.
- Kusky T, Li JH and Santosh M**, (2007) The Paleoproterozoic North Hebei Orogen: North China craton's collisional suture with the Columbia supercontinent. *Gondwana Research* **12**(1–2), 4–28.
- Kusky TM and Li JH**, (2003) Paleoproterozoic tectonic evolution of the North China Craton. *Journal of Asian Earth Sciences* **22**(4), 383–97.
- Lemaitre RW**, (1976) The Chemical Variability of some Common Igneous Rocks. *Journal of Petrology* **17**(4), 589–637.
- Li FQ, Zhang SZ, Li J, Liu H and Qin YD**, (2023b) Type and evolution of the Middle Jurassic–Early Cretaceous basin at the northern margin of the Lhasa Block: constraints of sedimentary characteristics and provenance tracing based on zircon U-Pb ages. Palaeoworld, available online.
- Li JY**, (2006) Permian geodynamic setting of Northeast China and adjacent regions: closure of the Paleo-Asian Ocean and subduction of the Paleo-Pacific Plate. *Journal of Asian Earth Sciences* **26**(3–4), 207–24.
- Li JY, Gao LM, Sun GH, Li YP and Wang YB**, (2007) Shuangjingzi middle Triassic syn-collisional crust-derived granite in the east Inner Mongolia and constraint on the timing of collision between Siberian and Sino-Korean paleo-plates. *Acta Petrologica Sinica* **23**(3), 565–82 (in Chinese with English abstract).
- Li M**, (2010) Crustal growth and evolution of Northeastern China as revealed by U-Pb age and Hf isotopes of detrital zircons from modern rivers. China University of Geoscience.
- Li SQ, Chen KF, Siebel W, Wu JD, Zhu XY, Shan XL and Sun XM**, (2012) Late Mesozoic tectonic evolution of the Songliao basin, NE China: Evidence from detrital zircon ages and Sr–Nd isotopes. *Gondwana Research* **22**(3–4), 943–55.
- Li W**, (2008) *The distribution characteristics and cause of soil anomalous elements at middle and lower reaches of the Second Songhua River*. Jilin University (in Chinese with English Abstract).
- Li WQ, Qian H, Xu PP, Hou K, Zhang QY, Chen Y, Chen J, Qu WG and Ren WH**, (2023a) Tracing sediment provenance in the Yellow River, China: Insights from weathering, recycling, and rock compositions. *Catena* **220**(Part B), 106727.
- Li Y, Xu WL, Zhang XM and Tang J**, (2024) Petrogenesis of Jurassic granitic plutons in the Yanbian area, NE China: Implications for the subduction history of the Paleo-Pacific Plate. *Journal of Asian Earth Sciences* **259**, 105940.
- Li Y, Xu WL, Zhou RX, Wang F, Ge WC and Sorokin AA**, (2020) Late Jurassic to early Early Cretaceous tectonic nature on the NE Asian continental margin: Constraints from Mesozoic accretionary complexes. *Earth-Science Reviews* **200**, 103042.
- Li YQ, Zhang DH, Sun XD and Lv CL**, (2019) Application of apatite fission-track analysis and zircon U-Pb geochronology to study the hydrothermal ore deposits in the Lesser Hinggan Range: Exhumation history and implications for mineral exploration. *Journal of Geochemical Exploration* **199**, 141–64.
- Liang ZW, Gao S, Hawkesworth CJ, Wu YB, Storey CD, Zhou L, Li M, Hu ZC, Liu YS and Liu XM**, (2018) Step-like growth of the continental crust in South China: evidence from detrital zircons in Yangtze River sediments. *Lithos* **320–321**, 155–71.
- Lim D, Jung H, Xu ZK, Jeong K and Li, T.G.**, (2015) Elemental and Sr–Nd isotopic compositional disparity of riverine sediments around the Yellow Sea: Constraints from grain-size and chemical partitioning. *Applied Geochemistry* **63**, 272–81.
- Lin X, Liu HJ, Liu J, Chen JX and Li LL**, (2022) The Yellow River did not enter the Bohai Bay basin during the Miocene: constraints from detrital zircon U-Pb age. *Acta Geologica Sinica* **96**(7), 2506–18 (in Chinese with English Abstract).
- Lin X, Liu J, Wu ZH, Wang SM, Zhao XT, Chen Y, Li ZN and Liu HJ**, (2020) Detrital zircon U-Pb ages and K feldspar main and trace elements provenance studying from fluvial to marine sediments in northern China. *Acta Geologica Sinica* **94**(10), 3024–35 (in Chinese with English Abstract).
- Liu BJ, Liu CQ, Zhang G, Zhao ZQ, Li SL, Hu J, Ding H, Lang YC, Li XD**, (2013) Chemical weathering under mid- to cool temperate and monsoon-controlled climate: A study on water geochemistry of the Songhuajiang River system, northeast China. *Applied Geochemistry* **31**, 265–78.
- Liu F, Guo JH, Lu XP and Diwu CR**, (2009) Nd–Hf isotope evidence for the 2.5 Ga crustal growth event in the North China Craton: A case study of the Hua'an gneiss terrane. *Science Bulletin* **54**(17), 2517–26 (in Chinese).
- Liu G, Lv XB, Chen C, Yang YS, Wang QJ and Sun YF**, (2014) Zircon U-Pb chronology and geochemistry of Mesozoic bimodal volcanic rocks from Nenjiang area in Da Hinggan Mountains and their tectonic implications. *Acta Petrologica et Mineralogica* **33**(3), 458–70 (in Chinese with English abstract).
- Liu JQ, Chen SS, Guo ZF, Gou WF, He HY, You HT, Kim HM, Sung GH and Kim H**, (2015) Geological background and geodynamic mechanism of Mt. Changbai volcanoes on the China–Korea border. *Lithos An International Journal of Mineralogy Petrology and Geochemistry* **236–237**, 46–73.
- Liu RX, Fan QC, Zheng XS, Zhang M and Li N**, (1998) Magmatic Evolution of the Changbai Mountain Tianchi Volcano. *Science in China (Series D)* **28**(03), 226–31 (in Chinese).
- Liu YJ, Li WM, Ma YF, Feng ZQ, Guan QB, Li SZ, Chen ZX, Liang CY and Wen, Q.B.**, (2021) An orocline in the eastern Central Asian Orogenic Belt. *Earth-Science Reviews* **221**(1), 103808.
- Liu YJ, Ma YF, Feng ZQ, Li WM, Li SZ, Guan QB, Chen ZX, Zhou T and Fang QA**, (2022) Paleozoic Orocline in the eastern Central Asian Orogenic Belt. *Acta Geologica Sinica* **96**(10), 3468–93 (in Chinese with English Abstract).
- Liyouck PR, Ngueutchoua G, Armstrong-Altrin JS, Sonfack AN, Ngagoum YSK, Bessa AZE, Bela VA, Tsanga DA and Wouatong ASL**, (2023) Petrography and geochemistry of the Sanaga river sediments, central Cameroon: Constraints on weathering, provenance, and tectonic setting. *Journal of African Earth Sciences* **199**, 104840.
- Ludwig KR**, (2003) ISOPLLOT 3.0: A Geochronological Toolkit for Microsoft Excel. Berkeley Geochronology Center Special Publication, 4.

- Lv CL, Xiao QH, Feng JL, Li XP, Deng CZ, Ren FH and Zheng WZ, (2015) The Discovery of Late Triassic–Early Jurassic Volcanic Rocks and Their Geological Implications in Northern Songnen Block. 29(4). Geoscience, Heilongjiang Province, pp. 855–865 (in Chinese).
- Lv J, Wang XG, Li Y and Ye L, (2017) Changes and optimal regulation of river and lake systems in the Songhua River basin. China Water Power Press, 1–123 (in Chinese).
- Ma Q and Xu YG, (2021) Magmatic perspective on subduction of Paleo-Pacific plate and initiation of big mantle wedge in East Asia. *Earth-Science Reviews* 213, 103473.
- Ma XT, (1987) *Lithospheric Dynamics Map of China and Adjacent Seas (1:4,000,000) and Explanatory Notes (in Chinese)*. Geological Publishing House, Beijing.
- Mange MA and Maurer HFW, (1992) *Heavy Minerals in Colour*. Chapman and Hall, 1–147.
- Mange MA and Wright TD, (2007) *Heavy Minerals in Use*. Elsevier, 1–1283.
- Marmo V, (1979) Granite Petrology and Granite Problems. Geological Publishing House, 1–255 (in Chinese).
- Matenco L and Andriessen P, (2013) Quantifying the mass transfer from mountain ranges to deposition in sedimentary basins: Source to sink studies in the Danube Basin–Black Sea system. *Global and Planetary Change* 103, 1–18.
- McLennan SM, Taylor SR and Eriksson KA, (1983) Geochemistry of Archean shales from the Pilbara Supergroup, Western Australia. *Geochimica et Cosmochimica Acta* 47(7), 1211–22.
- McLennan SM, Taylor SR, Mcculloch MT and Maynard JB, (1990) Geochemical and Nd–Sr isotopic composition of deep-sea turbidites: Crustal evolution and plate tectonic associations. *Geochimica et Cosmochimica Acta* 54(7), 2015–50.
- McLennan SM, (1993a) Weathering and Global Denudation. *Journal of Geology* 101(2), 295–303.
- McLennan SM, Hemming S, Mcdaniel DK and Hanson GN, (1993b) Geochemical approaches to sedimentation, provenance, and tectonics. *Processes Controlling the Composition of Clastic Sediments* 284, 21–40.
- Nesbitt HW, (1979) Mobility and fractionation of rare earth elements during weathering of granodiorite. *Nature* 279, 206–10.
- Nesbitt HW and Young GM, (1982) Early Proterozoic climates and plate motions inferred from major element chemistry of lutites. *Nature* 299, 715–17.
- Nesbitt HW and Young GM, (1984) Prediction of some weathering trends of plutonic and volcanic rocks based on thermodynamic and kinetic considerations. *Geochimica et Cosmochimica Acta* 48(7), 1523–34.
- Ohta T, (2008) Measuring and adjusting the weathering and hydraulic sorting effects for rigorous provenance analysis of sedimentary rocks: a case study from the Jurassic Ashikita Group, south-west Japan. *Sedimentology* 55, 1687–701.
- Ohta T and Arai H, (2007) Statistical empirical index of chemical weathering in igneous rocks: A new tool for evaluating the degree of weathering. *Chemical Geology* 240(3–4), 280–97.
- Parker A, (1970) An Index of Weathering for Silicate Rocks. *Geological Magazine* 107(6), 501–04.
- Pearce NJG, Perkins WT, Westgate JA, Gorton MP, Jackson SE, Neal CR and Chenerly SP, (1997) A compilation of new and published major and trace element data for NIST SRM 610 and NIST SRM 612 glass reference materials. *Geostandards Newsletter* 21(1), 115–44.
- Perri F, Dominici R, Pera EL, Chiocci FL and Martorelli E, (2016) Holocene sediments of the Messina Strait (southern Italy): relationships between source area and depositional basin. *Marine and Petroleum Geology* 77, 553–56.
- Pettijohn FJ, Potter PE and Siever R, (1987) *Sand and Sandstone*. Berlin Heidelberg: Springer-Verlag, 1–553.
- Qiao ZK, Huang DN, Zhou WY and Gao XH, (2016) Research of geological structure of Changbai mountain basalt cover. *Progress in Geophysics* 31(5), 1991–97 (in Chinese with English Abstract).
- Qiu SW, Wang XK, Makhinov AN, Yan BX, Lian Y, Zhu JH, Zhang FL and Zhang ZQ, (2014) Summary of the paleodrainage pattern changes in the Northeast China Plain and its neighboring areas. *Acta Geographica Sinica* 69(11), 1604–14 (in Chinese with English Abstract).
- Quek LX, Lee TY, Ghani, AA, Lai YM, Roselee MH, Lee HY, Iizuka Y, Lin YL, Yeh MW, Amran MA and Rahmat R, (2021) Tracing detrital signature from Indochina in Peninsular Malaysia fluvial sediment: Possible detrital zircon recycling into West Borneo Cenozoic sediments. *Journal of Asian Earth Sciences* 218, 104876.
- Rao WB, Chen J, Tan HB, Jiang SY and Su J, (2011) Sr–Nd isotopic and REE geochemical constraints on the provenance of fine-grained sands in the Ordos deserts, north-central China. *Geomorphology* 132(3–4), 123–38.
- Rao WB, Yang JD, Chen J and Li GJ, (2006) Sr–Nd isotope geochemistry of eolian dust of the arid-semiarid areas in China: Implications for loess provenance and monsoon evolution. *Science Bulletin* 51(12), 1401–12.
- Ren Q, Zhang SH, Sukhbaatar T, Hou MC, Wu HC, Yang TS, Li HY and Chen AQ, (2023) Timing the Hegenshan Suture in the Central Asian Orogenic Belt: New Paleomagnetic and Geochronological Constraints From Southeastern Mongolia. *Geophysical Research Letters* 50(20), 1–11.
- Roddaz M, Christophoul F, Zambrano JDB, Soula JC and Baby P, (2012) Provenance of late Oligocene to quaternary sediments of the Ecuadorian Amazonian foreland basin as inferred from major and trace element geochemistry and Nd–Sr isotopic composition. *Journal of South American Earth Sciences* 37, 136–53.
- Roser BP, Cooper RA, Nathan S and Tulloch AJ, (1996) Reconnaissance sandstone geochemistry, provenance, and tectonic setting of the lower Paleozoic terranes of the West Coast and Nelson, New Zealand. *New Zealand Journal of Geology and Geophysics* 39(1), 1–16.
- Roser BP, Korsch RJ, (1986) Provenance signatures of sandstone-mudstone suite determined using discriminant function analysis of major element data. *Chemical Geology* 67, 119–39.
- Rudnick RL and Gao S, (2003) *Treatise on Geochemistry (Second Edition)*. Elsevier, 1–64.
- Saha A, Roy DK, Khan R, Ornee TI, Goswami S, Idris AM, Biswas PK and Tamim U, (2023) Provenance, weathering, climate and tectonic setting of Padma River sediments, Bangladesh: A geochemical approach. *Catena* 233, 107485.
- Schneider S, Hornung J, Hinderer M and Garzanti E, (2016) Petrography and geochemistry of modern river sediments in an equatorial environment (Rwenzori Mountains and Albertine rift, Uganda) — Implications for weathering and provenance. *Sedimentary Geology* 336, 106–19.
- Sengör AMC, Natal'in BA and Burtman VS, (1993) Evolution of the Altaid tectonic collage and Palaeozoic crustal growth in Eurasia. *Nature* 364, 22.
- Shao JA, Li YF and Tang KD, (2013) Restoration of the orogenic processes of Zhangguangcai Range. *Acta Petrologica Sinica* 29(9), 2959–70 (in Chinese with English Abstract).
- Shao JQ, Yang SY and Li C, (2012) Chemical indices (CIA and WIP) as proxies for integrated chemical weathering in China: Inferences from analysis of fluvial sediments. *Sedimentary Geology* 265–266, 110–20.
- Shen QH, Geng YS, Song B and Wan YS, (2005) New information from the surface outcrops and deep crust of Archean rocks of the North China and Yangtze Blocks, and Qinling-Dabie Orogenic Belt. *Acta Geologica Sinica* 75 (5), 616–27 (in Chinese with English abstract).
- Shen QH, Wu JS and Geng YS, (1999) Evolutionary Stages of the Archaean continental crust in China. *Geoscience*, 2, 193–194 (in Chinese).
- Siebert L, Simkin TS and Kimberly P, (2010) *Volcanoes of the World*. Hutchinson Ross Pub Co., 1–551.
- Singh P., (2009) Major, trace and REE geochemistry of the Ganga River sediments: Influence of provenance and sedimentary processes. *Chemical Geology* 266(3–4), 242–55.
- Sláma J, Košler J, Condon DJ, Crowley JL, Gerdes A, Hanchar JM, Horstwood MSA, Morris GA, Nasdala L, Norberg N, Schaltegger, U, Schoene B, Tubrett MN and Whitehouse MJ, (2008) Plešovice zircon — A new natural reference material for U–Pb and Hf isotopic microanalysis. *Chemical Geology* 249(1–2), 1–35.
- Song WM, Du JY, Na FC, Pang XJ, Yang JL, Liu YC, Sun W, Tao N and Ge JT, (2019) Zircon U–Pb dating and petrogenesis of Early Cretaceous alkaline rhyolites in Tuquan Basin of middle Da Hinggan Mountains. *Geological Bulletin of China* 38(4), 619–31 (in Chinese with English abstract).

- Song WW, Zhou JB, Guo XD and Li YK, (2012) Geotectonic setting of Songliao block: reattribution from Paleozoic detrital zircon U–Pb dating. *Global Geology* 31(3), 522–35 (in Chinese with English abstract).
- Sun DY, Suzuki K, Wu FY and Lu XP, (2005) CHIME dating and its application for Mesozoic granites of Huanggoushan, Jilin Province. *Geochimica* 34(4), 305–14 (in Chinese with English abstract).
- Sun L, Xie YY, Kang CG, Chi YP, Du HR and Wang JX, (2021) Heavy minerals, Sr–Nd isotopic composition of sandy land in Hulun Buir, Inner Mongolia and their implications for Asian aeolian dust system. *Geology in China* 48(6), 1965–74 (in Chinese with English Abstract).
- Sun LX, Chen XG, Wu DD, Liu LH, Jin GR and Wei, XQ, (2022) Provenance of sediments from the Niger Delta, Gulf of Guinea: Evidence from geochemistry. *Journal of Marine Systems* 235, 103794.
- Tang J, Xu WL, Wang F and Ge WC, (2018a) Subduction history of the Paleo-Pacific slab beneath Eurasian continent: Mesozoic–Paleogene magmatic records in Northeast Asia. *Science China Earth Sciences* 61, 527–59.
- Tang ZY, Sun DY, Mao AQ, Yang DG and Deng CZ, (2018b) Timing and evolution of Mesozoic volcanism in the central Great Xing’an Range, northeastern China. *Geological Journal* 54(6), 3737–54.
- Taylor SG and Bradley CE, (1985) Optimal Ordering Strategies for Announced Price Increases. *Operations Research* 33(2), 312–25.
- Taylor SR and McLennan SM, (1985) *The Continental Crust: Its Composition and Evolution*. Blackwell Scientific, Oxford.
- Tobia FH, Al-Jaleel HS and Ahmad I, (2019) Ahmad, I.N., Provenance and depositional environment of the Middle-Late Jurassic shales, northern Iraq. *Geosciences Journal* 23, 747–65.
- Tribouillard N, Algeo TJ, Lyons T and Riboulleau A, (2006) Trace metals as paleoredox and paleoproductivity proxies: An update. *Chemical Geology* 232(1–2), 12–32.
- Újvári, G., Varga, A., Ramos, F.C., Kovács, J., Németh, T. and Stevens, T., (2012) Evaluating the use of clay mineralogy, Sr–Nd isotopes and zircon U–Pb ages in tracking dust provenance: An example from loess of the Carpathian Basin. *Chemical Geology* 304–305, 83–96.
- Verma SP and Armstrong-Altrin JS, (2016) Geochemical discrimination of siliciclastic sediments from active and passive margin settings. *Sedimentary Geology* 332, 1–12.
- Walsh JP, Wiberg PL, Aalto R, Nittrouer CA and Kuehl SA, (2016) Source-to-sink research: economy of the Earth’s surface and its strata. *Earth-Science Reviews* 153, 1–6.
- Walter HJ, Hegner E, Diekmann B, Kuhn G and Rutgers van der loeff MM, (2000) Provenance and transport of terrigenous sediment in the south Atlantic Ocean and their relations to glacial and interglacial cycles: Nd and Sr isotopic evidence. *Geochimica et Cosmochimica Acta* 64(22), 3813–27.
- Wan YS, Dong, C.Y., Xie HQ, Wang SJ, Song MC, Xu ZY, Wang SY, Zhou HY, Ma MZ and Liu DY, (2012) Formation ages of Early Precambrian BIFs in the North China Craton: SHRIMP zircon U–Pb dating. *Acta Geologica Sinica* 86(9), 1447–78 (in Chinese with English abstract).
- Wan YS, Dong CY, Ren P, Bai WQ, Xie HQ, Liu SJ, Xie SW and Liu DY, (2017) Spatial and temporal distribution, compositional characteristics and formation and evolution of Archean TTG rocks in the North China Craton: A synthesis. *Acta Petrologica Sinica* 33(5), 1405–19 (in Chinese with English abstract).
- Wan YS, Liu DY, Dong CY, Xie HQ, Kröner A, Ma MZ, Liu SJ, Xie SW and Ren P, (2015) Formation and evolution of Archean continental crust of the North China Craton. In: MG Zhai, ed. *Precambrian Geology of China*. Berlin Heidelberg: Springer, 59–136.
- Wan YS, Liu DY, Xu ZY, Dong CY, Wang ZJ, Zhou HY, Yang ZS, Liu ZH and Wu JS, (2008) Paleoproterozoic crustally derived carbonate-rich magmatic rocks from the Daqinshan area, North China Craton: Geological, petrographical, geochronological and geochemical (Hf, Nd, O and C) evidence. *American Journal of Science* 308(3), 351–78.
- Wan YS, Song B, Liu DY, Li HM, Yang C, Zhang QD, Yang CH, Geng YS and Shen QH, (2001) Geochronology and geochemistry of 3.8–2.5 Ga ancient rock belt in the Dongshan Scenic Park, Anshan area. *Acta Geologica Sinica* 3, 363–70 (in Chinese with English abstract).
- Wan YS, Xie HQ, Dong CY and Liu DY, (2020) Timing of tectonothermal events in Archean basement of the North China Craton. *Earth Science* 45(9), 3119–60 (in Chinese with English abstract).
- Wan YS, Xie HQ, Wang HC, Li PC, Chu H, Xiao ZB, Dong CY, Liu SJ, Li Y, Hao GM and Liu DY, (2021b) Discovery of ~ 3.8Ga TTG rocks in eastern Hebei, North China Craton. *Acta Geologica Sinica* 95(5), 1321–33 (in Chinese with English abstract).
- Wan YS, Xie HQ, Wang HC, Liu SJ, Chu H, Xiao ZB, Li Y, Hao GM, Li PC, Dong CY and Liu DY, (2021a) Discovery of early Eoarchean–Hadean zircons in eastern Hebei, North China Craton. *Acta Geologica Sinica* 95(2), 277–91 (in Chinese with English abstract).
- Wang CL, Zhang LC, Dai YP and Lan GY, (2015b) Geochronological and geochemical constraints on the origin of clastic meta-sedimentary rocks associated with the Yuanjiacun BIF from the Lüliang Complex, North China. *Lithos* 212–215, 231–46.
- Wang F, Xu WL, Meng E, Cao HH and Gao FH, (2012) Early Paleozoic amalgamation of the Songnen–Zhangguangcai Range and Jiamusi massifs in the eastern segment of the Central Asian Orogenic Belt: Geochronological and geochemical evidence from granitoids and rhyolites - ScienceDirect. *Journal of Asian Earth Sciences* 49, 234–48.
- Wang F, Xu WL, Xu YG, Gao FH and Ge WC, (2015c) Late Triassic bimodal igneous rocks in eastern Heilongjiang Province, NE China: Implications for the initiation of subduction of the Paleo-Pacific Plate beneath Eurasia. *Journal of Asian Earth Sciences* 97(Part B), 406–23.
- Wang FB and Yang YC, (2019) Geochemistry, zircon U–Pb ages and geological significance of volcanic rocks from Shangmachang gold deposit, Northern Da Hinggan Mountains. *Mineral Deposits*, 38(3), 571–85 (in Chinese with English abstract).
- Wang HQ, Hu B, Teng YG, Zhan YH and Zhai YZ, (2021) Mass concentrations and patterns of rare earth elements in groundwater of Lalin River basin. *South-to-North Water Transfers and Water Science and Technology* 19(1) 158–167. (in Chinese with English Abstract).
- Wang HZ and Mo XX, (1996) An outline of the tectonic evolution of China. *Episodes* 18, 1–2.
- Wang K, Li YL, Xiao WJ, Zheng JP, Wang C, Jiang H and Brouwer FM, (2024) Geochemistry and zircon U–Pb–Hf isotopes of Paleozoic granitoids along the Solonker suture zone in Inner Mongolia, China: constraints on bidirectional subduction and closure timing of the Paleo-Asian Ocean. *Gondwana Research* 126, 1–21.
- Wang SJ, Wang YJ, Ran LS. and Su T, (2015a) Climatic and anthropogenic impacts on runoff changes in the Songhua River basin over the last 56 years (1955–2010), Northeastern China. *Catena* 127, 258–69.
- Wang T, Guo L, Zhang L, Yang QD, Zhang JJ, Tong Y and Ye K, (2015d) Timing and evolution of Jurassic–Cretaceous granitoid magmatism in the Mongol–Okhotsk belt and adjacent areas, NE Asia: Implications for transition from contractional crustal thickening to extensional thinning and geodynamic settings. *Journal of Asian Earth Sciences* 97(Part B), 365–92.
- Wang T, Tong Y, Huang H, Zhang HR, Guo L, Li ZX, Wang XX, Eglinton B, Li S, Zhang JJ, Donskaya TV, Petrov O, Zhang L, Song P, Zhang XW and Wang CY, (2022) Granitic record of the assembly of the Asian continent. *Earth-Science Reviews* 237, 104298.
- Wang T, Zhu XM, Dong YL, Chen HH, Su B, Liu Y and Wu W, (2020) Trace elements as paleo sedimentary environment indicators: a case study of the Paleogene Anjihaihe Formation in the northwestern Junggar basin. *Acta Geologica Sinica* 94(12), 3830–51 (in Chinese with English Abstract).
- Wang Y, Li CF, Wei HQ and Shan XJ, (2003) Late Pliocene–recent tectonic setting for the Tianchi volcanic zone, Changbai Mountains, northeast China. *Journal of Asian Earth Sciences* 21(10), 1159–70.
- Wang Y, Zhang, FQ, Zhang DW, Miao LC, Li TS, Xie HQ, Meng QR and Liu DY, (2006) SHRIMP zircon U–Pb ages of diorite in the southern Songliao Basin and their geological significance. *Science Bulletin* 51(15), 1811–16 (in Chinese).
- Wang YH, Xie YY, Chi YP, Kang CG, Wu P, Sun L and Liu RN, (2023) Detrital zircon U–Pb age signatures of coarse-fine fractions in the Horqin sand land: Implications for quantitative provenance and regional tectonic-magmatic evolutionary events. *Acta Geologica Sinica* 97, 1–20 (in Chinese with English abstract).
- Wang YL, Wang LG and Zhai SF, (2019) On Lalin River Basin’s Geographical Environment and Its Early History and Culture. *Journal of Bohai University: Philosophy and Social Sciences Edition* 1, 28–32 (in Chinese with English Abstract).

- Wang YS, Du BY, Xu RK, Chen X, Sun SH, Lu LH, Hou WD and Cheng XZ, (2018) Zircon U-Pb dating, geochemistry and tectonic setting of the Mesozoic intermediate-acid volcanic rocks in Tayuan area, Greater Khingan Range. *Mineral Exploration*, 9(1), 22–32 (in Chinese with English abstract).
- Wang YX, Yang JD, Chen J, Zhang KJ and Rao WB, (2007) The Sr and Nd isotopic variations of the Chinese Loess Plateau during the past 7 Ma: Implications for the East Asian winter monsoon and source areas of loess. *Palaeogeography Palaeoclimatology Palaeoecology* 249(3–4), 351–61.
- Wang ZW, Pei FP, Xu WL, Cao HH, Wang ZJ and Zhang Y, (2016a) Tectonic evolution of the eastern Central Asian Orogenic Belt: Evidence from zircon U–Pb–Hf isotopes and geochemistry of early Paleozoic rocks in Yanbian region, NE China. *Gondwana Research* 38, 334–50.
- Wang ZW, Xu WL, Pei FP, Wang F and Guo P, (2016b) Geochronology and geochemistry of early Paleozoic igneous rocks of the Lesser Xing'an Range, NE China: Implications for the tectonic evolution of the eastern Central Asian Orogenic Belt. *Lithos* 261, 144–63.
- Weaver CE, (1989) *Clays, Muds, and Shales*. Elsevier, 1–819.
- Wei HQ, Liu GM and Gill J, (2013) Review of eruptive activity at Tianchi volcano, Changbaishan, northeast China: implications for possible future eruptions. *Bulletin of Volcanology* 75(706), 1–14.
- Wei HY, (2012) Geochronology and Petrogenesis of Granitoids in Yichun–Hegang Area, Heilongjiang Province. Jilin University, Changchun (in Chinese with English abstract).
- Weltje GJ and Eynatten, HV, (2004) Quantitative provenance analysis of sediments: review and outlook. *Sedimentary Geology* 171, 1–11.
- Wiedenbeck M, Allé P, Corfu F, Griffin WL, Meier M, Oberli F, Quadt AV, Roddick JC and Spiegel W, (1995) Three natural zircon standards for U–Th–Pb, Lu–Hf, trace element and REE analyses. *Geostandards Newsletter* 19, 1–23.
- Windley BF, (1995) *The Evolving Continents* (3rd Edition). Chichester: John Wiley & Sons, 1–526.
- Windley BF, Alexeiev D, Xiao WJ, Kröner A and Badarch G, (2007) Tectonic models for accretion of the Central Asian Orogenic Belt. *Journal of Geological Society* 164, 31–47.
- Wu FY, Sun DY, Ge WC, Zhang YB, Grant ML, Wilde SA and Jahn BM, (2011) Geochronology of the Phanerozoic granitoids in northeastern China. *Journal of Asian Earth Sciences* 41(1), 1–30.
- Wu FY, Sun DY, Li HM, Jahn BM and Wilde S, (2002) A-type granites in northeastern China: age and geochemical constraints on their petrogenesis. *Chemical Geology* 187, 143–73.
- Wu FY, Sun DY, Li HM and Wang XL, (2001) The Nature of Basement Beneath the Songliao Basin in NE China: Geochemical and Isotopic Constraints. *Physics and Chemistry of the Earth, Part A: Solid Earth and Geodesy* 26(9–10), 793–803.
- Wu FY, Yang JH, Lo CH, Wilde SM, Sun DY and Jahn BM, (2007b) The Heilongjiang Group: A Jurassic accretionary complex in the Jiamusi Massif at the western Pacific margin of Northeastern China. *Island Arc* 16(1), 156–72.
- Wu FY, Ye M and Zhang SH, (1994) Geodynamic model of the Manzhouli–Suifenhe geoscience transect. *Earth Science–Journal of China University of Geosciences* 20, 5 (in Chinese with English Abstract).
- Wu FY, Zhao, G.C., Sun, D.Y., Wilde, S.A. and Yang, J.H., (2007a) The Hulan Group: Its role in the evolution of the Central Asian Orogenic Belt of NE China. *Journal of Asian Earth Sciences* 30(3–4), 542–56.
- Wu P, Xie YY, Kang CG, Chi YP, Sun L and Wei ZY, (2022) Effects of Provenance, Transport Processes and Chemical Weathering on Heavy Mineral Composition: A Case Study from the Songhua River Drainage, NE China. *Frontiers in Earth Science* 10, 839745.
- Wu YB and Zheng YF, (2004) Genetic Mineralogy of zircons and its constraints on U–Pb age interpretation. *Science Bulletin* 49(16), 1589–604 (in Chinese).
- Xiao WJ, Windley BF, Hao J and Zhai MG, (2003) Accretion leading to collision and the Permian Solonker suture, Inner Mongolia, China: Termination of the central Asian orogenic belt. *Tectonics* 22(6), 1–20.
- Xiao WJ, Windley BF, Huang BC, Han CM, Yuan C, Chen HL, Sun M, Sun S and Li JL, (2009) End-Permian to mid-Triassic termination of the accretionary processes of the southern Altaids: implications for the geodynamic evolution, Phanerozoic continental growth, and metallogeny of Central Asia. *International Journal of Earth Sciences (Geol Rundsch)*, 98, 1189–217.
- Xie YY, Kang CG, Chi YP, Du HR, Wang JX and Sun L, (2019a) The loess deposits in Northeast China: The linkage of loess accumulation and geomorphic-climatic features at the easternmost edge of the Eurasian loess belt. *Journal of Asian Earth Sciences* 181, 103914.
- Xie YY, Kang CG, Chi YP, Wu P, Wei ZY, Wang JX and Sun L, (2020) Reversal of the middle-upper Songhua River in the late Early Pleistocene, Northeast China. *Geomorphology* 369, 107373
- Xie YY, Lu L, Kang CG and Chi YP, (2019b) Sr–Nd isotopic characteristics of the Northeast Sandy Land, China and their implications for tracing sources of regional dust - ScienceDirect. *Catena* 184, 104303.
- Xie YY, Yuan F, Zhan T, Kang CG and Chi YP, (2018a) Geochemical and isotopic characteristics of sediments from the HulunBuir Sandy Land, northeast China: implication for weathering, recycling and dust provenance. *Catena* 160, 170–84.
- Xie YY, Yuan F, Zhan T, Kang CG, Chi YP and Ma YF, (2018b) Geochemistry of loess deposits in northeastern China: constraint on provenance and implication for disappearance of the large Songliao palaeolake. *Journal of the Geological Society* 175(1), 146–62.
- Xu H, Liu B and Wu F, (2010) Spatial and temporal variations of Rb/Sr ratios of the bulk surface sediments in Lake Qinghai. *Geochemical Transactions* 11(1), 1–8.
- Xu WL, Pei FP, Wang F, Meng E, Ji WQ, Yang DB and Wang W, (2013) Spatial–temporal relationships of Mesozoic volcanic rocks in NE China: Constraints on tectonic overprinting and transformations multiple tectonic regimes. *Journal of Earth Sciences* 74, 167–93.
- Yang BJ, Mu SM, Jin X and Liu C, (1996) Synthesized study on the geophysics of Manzhouli–Suifenhe Geoscience transect, China. *Acta Geophysica Sinica* 39(6), 772–82 (in Chinese with English abstract).
- Yang H, Ge WC, Zhao GC, Dong Y, Xu WL, Wang ZH, Ji Z and Yu JJ, (2015) Late Triassic intrusive complex in the Jidong region, Jiamusi–Khanka Block, NE China: geochemistry, zircon U–Pb ages, Lu–Hf isotopes, and implications for magma mingling and mixing. *Lithos* 224–225, 143–59.
- Yang H, Ge WC, Zhao GC, Yu JJ and Zhang YL, (2014) Early Permian–late Triassic granitic magmatism in the Jiamusi–Khanka Massif, eastern segment of the Central Asian Orogenic Belt and its implications. *Gondwana Research* 27 (4), 1509–33.
- Yang SY, Wang ZB, Guo Y, Li CX and Cai JG, (2009) Heavy mineral compositions of the Changjiang (Yangtze River) sediments and their provenance-tracing implication. *Journal of Asian Earth Sciences* 35, 56–65.
- Yang SY, Yim WS and Huang, GQ, (2008) Geochemical composition of inner shelf Quaternary sediments in the northern South China Sea with implications for provenance discrimination and paleoenvironmental reconstruction. *Global and Planetary Change* 60(3–4), 207–21.
- Yang SY, Zhang F and Wang ZB, (2012) Grain size distribution and age population of detrital zircons from the Changjiang (Yangtze) River system, China. *Chemical Geology* 296–297, 26–38.
- Zang YH, Li JM, Ning J. and Wang HT, (2023) Provenance and tectonic setting of the Upper Cretaceous Yaojia Formation sandstones in the Hailijin area, southern Songliao Basin: Constraints from petrogeochemistry and zircon U–Pb chronology. *Bulletin of Geological Science and Technology* 42(5), 175–90 (in Chinese with English abstract).
- Zhai MG, (2010) Tectonic evolution and metallogeny of North China Craton. *Mineral Deposits*, 29(1), 24–36. (in Chinese with English abstract).
- Zhai MG and Bian AG, (2000) The Late Neoproterozoic to Middle Proterozoic Splitting of the North China Craton. *Science in China (Series D)*, 30, 129–37 (in Chinese).
- Zhang GB, Chen XK, Zhao Y, Tang JY, Li RR, Feng Y and Kong JG, (2022b) Geochronology, Geochemistry and Geological significance of the middle Jurassic Porphyritic Monzogranite in the Southern Zhangguangcai range, Heilongjiang Province. *Journal of Jilin University (Earth Science Edition)* 52(6), 1907–25 (in Chinese with English Abstract).
- Zhang HT, Zhang XZ, Zeng Z, Liu Y and Cui WL, (2017) Geochronological and geochemical characteristics of Neoproterozoic basement under Conozoic basalt in Changbai Mountain. *Global Geology* 36(3), 763–76 (in Chinese with English abstract).

- Zhang HZ, Lu HY, Zhou YL, Cui YY, Zhang J and Lv F, Chen ZY** (2022a) Quantitative analysis of the clastic mineral composition in sediments from the Weihe River basin by scanning electron microscope and its implication for provenance. *Acta Sedimentologica Sinica*, **40**(4), 944–56 (in Chinese with English Abstract).
- Zhang J, Geng HP, Pan BT, Hu XF, Chen LP, Wang W, Chen DB and Zhao QM** (2020) Climatic zonation complicated the lithology controls on the mineralogy and geochemistry of fluvial sediments in the Heihe River basin, NE Tibetan Plateau. *Quaternary International*, **537**, 33–47.
- Zhang J, Wan SM, Clift PD, Huang J, Yu ZJ, Zhang KD, Mei X, Liu J, Han ZY, Nan QY, Zhao DB, Li AC, Chen LH, Zheng HB, Yang SY, Li TG and Zhang XH**, (2019b) History of Yellow River and Yangtze River delivering sediment to the Yellow Sea since 3.5 Ma: tectonic or climate forcing? *Quaternary Science Review* **216**, 74–88.
- Zhang XY, He MY, Wang B, Clift PD, Rits D**, (2019a) Provenance evolution of the northern Weihe Basin as an indicator of environmental changes during the Quaternary. *Geological Magazine* **156**(11), 1915–23.
- Zhang YJ, Wu XW, Jiang B, Guo W, Yang YJ, Liu SW, Cui TR, Li W, Li LC, Si QL and Zhang C**, (2015) U-Pb Geochronology of Detrital Zircon and the Constraint of Geochemistry from the Gegen'aobao Formation in Middle of Zalantun Area of Da Hinggan Mountains and Its Tectonic Significance. *Journal of Jilin University: Earth Science Edition* **45**(2), 404–16 (in Chinese with English abstract).
- Zhao D, Ge WC, Yang H, Dong Y, Bi JH and He Y**, (2018) Petrology, geochemistry, and zircon U–Pb–Hf isotopes of Late Triassic enclaves and host granitoids at the southeastern margin of the Songnen–Zhangguangcai Range Massif, Northeast China: Evidence for magma mixing during subduction of the Mudanjiang oceanic plate. *Lithos* **312–313**, 358–74.
- Zhao GC, Sun M, Wilde SA and Li SZ**, (2005) Late Archean to Paleoproterozoic evolution of the North China Craton: key issues revisited. *Precambrian Research* **136**(2), 177–202.
- Zhao GC, Wilde SA, Cawood PA and Sun M**, (2001) Archean blocks and their boundaries in the North China Craton: lithological, geochemical, structural and P–T path constraints and tectonic evolution. *Precambrian Research* **107**(1–2), 45–73.
- Zhao HY, Xie YY, Chi YP, Kang CG, Wu P, Sun L and Wei ZY**, (2023) Effects of Fluvial Processes on Sediment Geochemistry and Heavy Mineral Composition in a Small Catchment: A case study of the Balan River. *Acta Sedimentologica Sinica* 1–18 (in Chinese with English Abstract).
- Zheng HB, Clift PD, Wang P, Tada R, Jia JT, He MY and Jourdan F**, (2013) Pre-Miocene birth of the Yangtze River. *Acta Geologica Sinica (English edition)* **110**(19), 7556–61.
- Zhou M, Yu ZB**, (1984) Atlas of Environmental Quality Research of the Second Songhua River. Science Press, 1–74 (in Chinese).